Stem Cell Reports
Article

OPEN ACCESS

Activin/Nodal Signaling Supports Retinal Progenitor Specification in a Narrow Time Window during Pluripotent Stem Cell Neuralization

Michele Bertacchi,[1,10,11,12] Giuseppe Lupo,[2,3,4] Luca Pandolfini,[1] Simona Casarosa,[5] Mara D'Onofrio,[6,7] Roger A. Pedersen,[8] William A. Harris,[4] and Federico Cremisi[1,9,*]

[1]Laboratorio di Biologia, Scuola Normale Superiore di Pisa, Piazza dei Cavalieri 7, 56124 Pisa, Italy
[2]Department of Chemistry, Sapienza University of Rome, Piazzale A. Moro 5, 00185 Rome, Italy
[3]Istituto Pasteur-Fondazione Cenci Bolognetti, Sapienza University of Rome, Piazzale A. Moro 5, 00185 Rome, Italy
[4]Department of Physiology, Development and Neuroscience, University of Cambridge, Downing Street, Cambridge CB2 3DY, UK
[5]Centre for Integrative Biology, University of Trento, Via delle Regole 101, 38123 Mattarello (Trento), Italy
[6]Genomics Facility, European Brain Research Institute "Rita Levi-Montalcini," Via del Fosso di Fiorano 64, 00143 Rome, Italy
[7]Istituto di Farmacologia Traslazionale, CNR, Via del Fosso del Cavaliere 100, 00133 Rome, Italy
[8]Department of Surgery and The Anne McLaren Laboratory for Regenerative Medicine, Wellcome Trust-Medical Research Council Cambridge Stem Cell Institute, West Forvie Building, Robinson Way, Cambridge CB2 0SZ, UK
[9]Institute of Biomedical Technologies (ITB), National Research Council (CNR) of Pisa, Via Moruzzi 1, 56124 Pisa, Italy
[10]Present address: University of Nice Sophia-Antipolis, iBV, UMR 7277, 06108 Nice, France
[11]Present address: Inserm, iBV, U1091, 06108 Nice, France
[12]Present address: CNRS, iBV, UMR 7277, 06108 Nice, France
*Correspondence: federico.cremisi@sns.it
http://dx.doi.org/10.1016/j.stemcr.2015.08.011

SUMMARY

Retinal progenitors are initially found in the anterior neural plate region known as the eye field, whereas neighboring areas undertake telencephalic or hypothalamic development. Eye field cells become specified by switching on a network of eye field transcription factors, but the extracellular cues activating this network remain unclear. In this study, we used chemically defined media to induce in vitro differentiation of mouse embryonic stem cells (ESCs) toward eye field fates. Inhibition of Wnt/β-catenin signaling was sufficient to drive ESCs to telencephalic, but not retinal, fates. Instead, retinal progenitors could be generated from competent differentiating mouse ESCs by activation of Activin/Nodal signaling within a narrow temporal window corresponding to the emergence of primitive anterior neural progenitors. Activin also promoted eye field gene expression in differentiating human ESCs. Our results reveal insights into the mechanisms of eye field specification and open new avenues toward the generation of retinal progenitors for translational medicine.

INTRODUCTION

The vertebrate retina originates from the eye field, an anterior neural plate region identified by coexpression of a network of eye field transcription factors (EFTFs) including, among others, *Rax* and *Pax6* (Viczian, 2013).

In vertebrate embryos, downregulation of the bone morphogenetic protein (BMP) and Activin/Nodal signaling pathways is responsible for the specification of forebrain progenitors (Andoniadou and Martinez-Barbera, 2013). Anterior-posterior gradients of Wnts, fibroblast growth factors, and retinoic acid impose diencephalic, midbrain, hindbrain, or spinal cord identities on posteriorly located neural precursors. Rostral forebrain fates, instead, are preserved in anterior regions by shielding them from these signals (Andoniadou and Martinez-Barbera, 2013; Wilson and Houart, 2004).

Although diversification of the secondary prosencephalon into telencephalon, eye field, and hypothalamus has been difficult to dissect in vivo, it can be modeled in vitro using mouse and human embryonic stem cells (mESCs and hESCs, respectively). In these culture systems, both endogenous and exogenous signals contribute to cell-fate specification. Previous reports have shown induction of hypothalamic fates by minimizing ESC exposure to exogenous signals (Wataya et al., 2008), whereas culture in minimal media in the presence of transforming growth factor β and Wnt pathway inhibitors causes telencephalic specification (Bertacchi et al., 2015; Lupo et al., 2014). Extracellular cues, instead, appear to be critical for the induction of eye field fates, because production of retinal progenitors was generally inefficient in ESC systems with reduced extracellular signaling (Lupo et al., 2014).

Previous studies suggested that Activin/Nodal signaling promotes eye field fates, as shown by enhanced retinal progenitor generation in mESCs treated with exogenous Activin (Ikeda et al., 2005) and by repression of eye field gene expression in hESCs differentiating in the presence of Activin/Nodal pathway inhibitors (Lupo et al., 2013). The contribution of Activin/Nodal signaling to eye field specification, however, remains poorly understood (Lupo et al., 2014; Viczian, 2013). Here, building on previous studies (Ikeda et al., 2005; Lupo et al., 2013), we provide much more extensive evidence that Activin supports retinal identity in ESCs. Notably, we show that this function is restricted to a narrow time window coincident with the emergence of early

forebrain progenitors from pluripotent cells. These findings suggest the feasibility of efficiently mimicking retinal progenitor formation in vitro using purely defined reagents.

RESULTS

Activin Supports Expression of Eye Field Genes in mESCs Differentiating to Anterior Neural Progenitors

We recently described a protocol of mESC neuralization using a chemically defined minimal medium (CDMM) (Bertacchi et al., 2013). mESCs are prompted to differentiate by floating aggregate culture (step I, 2 days) and then allowed to spontaneously neuralize as adherent cultures (step II, 4–6 days). In these conditions, mESCs efficiently convert to neural progenitors, which can undergo neuronal differentiation following long-term culture (Bertacchi et al., 2013, 2015).

With this protocol, we found that the endogenous levels of extracellular signaling pathways in early differentiating mESCs are permissive for neural conversion. Emerging neural progenitors, however, produce BMP and Wnt signals that repress rostral forebrain specification and promote caudal forebrain/midbrain fates (Bertacchi et al., 2013, 2015). Because BMP-dependent caudalization is, at least in part, indirectly due to activation of Wnt signaling, treatments with Wnt/β-catenin inhibitors during step II are sufficient to elicit rostral forebrain character in mESCs (Figures 1A–1C; Bertacchi et al., 2015). In this study, we used this experimental system and a *Rax*-GFP knockin mESC line (K/l EB5), driving eGFP expression under control of the *Rax* promoter (Wataya et al., 2008), to investigate the signals promoting eye field fates in early anterior neural progenitors. mESCs were differentiated to neuroectoderm with or without the Wnt/β-catenin signaling inhibitor IWR-1-Endo (Wnti) applied from 3 days of in vitro differentiation (3 DIV) (Figure 1A). Cells were harvested every 12 hr between 3.5 and 10 DIV, and GFP-positive cells were detected by flow cytometry or immunostaining. Cells treated with Wnti showed a transient activation of GFP expression between 5 and 6 DIV (Figures 1B and 1D). GFP-positive cells then decreased, reaching the very low numbers seen in control cultures by 8 DIV (Figures 1B and 1E). By quantitative RT-PCR (qRT-PCR), a peak of eye field marker (*Rax*, *Six6*) transcription was detectable at 5 DIV, but it rapidly declined (Figure 1C). Instead, telencephalic markers (*Emx2*, *FoxG1*, *Tbr1*, *Ctip2*) were steadily upregulated from 5 DIV onward (Figure 1C). Thus, differentiation in the presence of Wnt/β-catenin inhibitors converts mESCs to early forebrain progenitors that are competent to express both eye field and telencephalic genes. In the absence of appropriate signals, however, eye field gene transcription is not maintained and telencephalic fates prevail.

Previous work described repression of eye field genes in adherent hESC cultures differentiating in the presence of inhibitors of Activin/Nodal signaling (Lupo et al., 2013). Furthermore, exogenous Activin enhances generation of retinal progenitors in mESCs cultured as floating aggregates in serum-containing media (Ikeda et al., 2005). Notably, bioinformatic analysis of chromatin immunoprecipitation sequencing datasets obtained in mouse and human ESCs indicate that both SMAD2/3 and FOXH1, key components of the Activin/Nodal pathway (Yamamoto et al., 2001), can bind to a highly conserved region located within 2 kb upstream of the *Rax* transcription start site (Figure S1; Kim et al., 2011; Mullen et al., 2011). Thus, the instability of eye field gene transcription in our differentiation system may be due to insufficient activation of Activin/Nodal signaling.

mESCs differentiating to neuroectoderm with our protocol show very low expression of Activin/Nodal ligands, suggesting that Activin/Nodal signaling remains quiescent in these conditions (Bertacchi et al., 2015). Confirming these data, we found that *FoxH1* was barely expressed in either control differentiation conditions or in the presence of Wnti and/or the BMP pathway inhibitor dorsomorphin (BMPi) at 6 DIV but was upregulated by treatments with exogenous Activin (10–100 ng/ml; Figures S2A and S2B). In these assays, weaker upregulation of *FoxH1* in the presence of BMPi (Figure S2B) is likely due to the previously described partial interference of BMPi with the Activin/Nodal pathway (Zhou et al., 2010). As previously described (Besser, 2004), high doses of Activin (50–100 ng/ml) also upregulated *Lefty1/2*, which encode for feedback inhibitors of Activin/Nodal signaling (Meno et al., 1999; Perea-Gomez et al., 2002), whereas genes encoding for other antagonists of this pathway (*Fst*; Hemmati-Brivanlou et al., 1994) were not affected (Figure S3B).

In support of the idea that Activin/Nodal signaling needs to be active for stable eye field gene transcription, simultaneous delivery of both Activin (10 ng/ml) and Wnti during mESC forebrain differentiation (Figure 1A; Figure S1C) increased the fraction of *Rax*-GFP-positive cells at 8–10 DIV compared to cultures treated with Wnti alone (Figures 1B and 1D–1F). Costaining with PAX6 suggested that *Rax*-GFP-positive cells had a retinal progenitor identity (Figures 1G and 1G′). By qRT-PCR at 8 DIV, cultures treated with both Activin and Wnti showed upregulation of eye field markers (*Otx2*, *Six3*, *Rax*, *Six6*, *Tbx3*, *Vsx2*) and downregulation of telencephalic markers (*FoxG1*, *Emx2*, *Tbr1*, *Ctip2*) in comparison with Wnti-treated samples (Figure 1H).

In time course assays, the percentage of *Rax*-GFP-positive cells in Activin-treated cultures, compared to samples treated with Wnti only, was lower at 5–6 DIV and became similar at 6.5 DIV (Figure 1B). From 6.5 DIV, however,

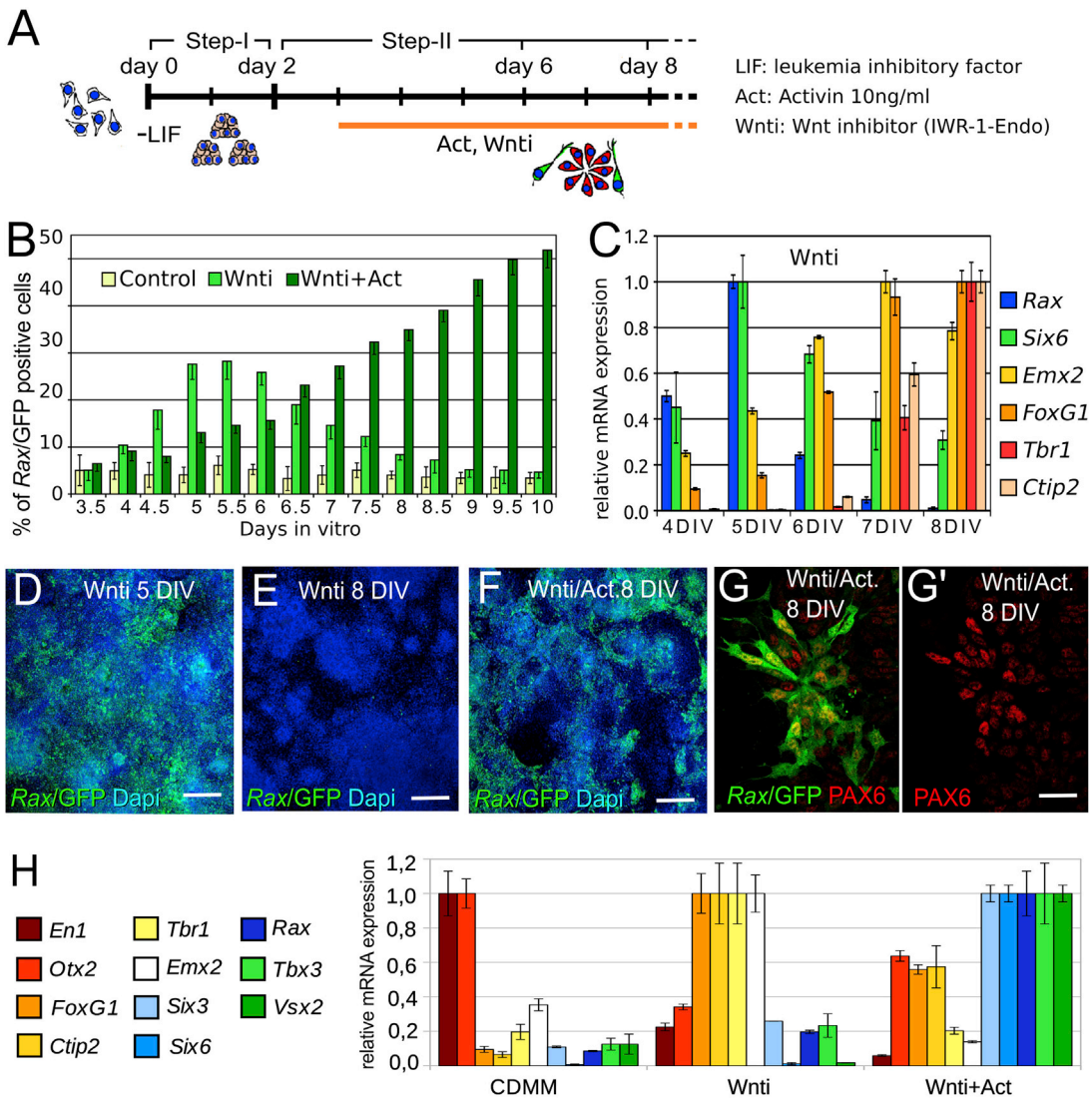

Figure 1. Activin Supports *Rax* Expression in mESC-Derived Early Anterior Neural Progenitors

(A) Scheme of mESC neuroectoderm differentiation with or without Wnti and Activin. Days show the time of mouse ESC differentiation after LIF (−LIF) and serum withdrawal.

(B) Flow cytometry of K/l EB5 cells harvested at different time points showing the percentage of *Rax*-GFP-positive cells during differentiation in plain CDMM (control) or in the presence of Wnti or Wnti and Activin (Wnti+Act), as indicated. Error bars represent SEM (n = 4 independent experiments with n = 3 in vitro technical replicates per experiment; technical replicates were pooled together and analyzed by n = 3 flow cytometry acquisitions).

(C) qRT-PCR quantification of telencephalic (*Emx2*, *FoxG1*, *Tbr1*, *Ctip2*) and eye field (*Rax*, *Six6*) gene expression in cells differentiated in the presence of Wnti and harvested every 24 hr between 4 and 8 DIV. For each analyzed gene, the sample with maximal transcription levels was chosen for normalization, and relative expression levels in all the other samples are shown. Error bars were obtained from the error propagation formula (n = 3 independent biological replicates were pooled together and analyzed by qRT-PCR).

(D–F) GFP immunodetection of cells differentiated in the presence of Wnti or Wnti and Activin (Wnti/Act.). The scale bars represent 50 μm. Dapi, 4′,6-diamidino-2-phenylindole.

(G and G′) Double immunodetection at 8 DIV in cultures treated with Wnti and Activin. The scale bar represents 10 μm.

(H) qRT-PCR of mesencephalic (*En1*, *Otx2*), telencephalic (*Emx2*, *FoxG1*, *Ctip2*, *Tbr1*), and eye field (*Rax*, *Six6*, *Vsx2*, *Six3*, *Otx2*, *Tbx3*) marker expression at 8 DIV in cultures differentiated in control medium (CDMM) or in medium supplemented with Wnti (Wnti) or both Wnti and Activin (10 ng/ml; Wnti+Act). Error bars were obtained from the error propagation formula (n = 3 independent experiments were pooled together and analyzed by qRT-PCR; each experiment contained n = 2 in vitro technical replicates).

See also Figures S1 and S2.

Rax-GFP-positive cells rapidly disappeared in Wnti-treated cultures, whereas their fraction progressively increased in the presence of Activin, nearly reaching 50% at 10 DIV (Figure 1B). Activin treatment delayed mESC neuralization, as shown by enhanced expression of the epiblast markers *Oct4* and *Fgf5* and repression of the neuroectoderm markers *Pax6* and *NCAM* at 6 DIV compared to controls (Figure S2D), thus explaining the later appearance of *Rax*-GFP-positive cells in Activin-treated cultures. Nonetheless, *Oct4* and *Fgf5* were downregulated at 8 DIV (Figure S2D) and neural progenitors expressing *Rax*-GFP, *Pax6*, and other eye field markers (e.g., *Six3*, *Six6*, *Tbx3*) became evident (Figures S2E–S2H). Thus, low doses of Activin can transiently delay neural differentiation in mESCs but, once cells convert to neural progenitors, Activin signaling can steer them toward eye field fates.

We systematically analyzed the effects of Activin/Nodal signaling on neural induction and patterning in mESCs, starting by treating differentiating cells with exogenous Activin at different concentrations. We delivered Activin and Wnti simultaneously from 3 DIV using 10, 50, and 100 ng/ml Activin (Figure S3). Activin caused dose-dependent inhibition of neural progenitor markers (*Sox2*, *Nestin*, *Pax6*, *Musashi*) and upregulation of pluripotency (*Oct4*, *Fgf5*) and mesendoderm (*Gata4*, *Gata6*) markers at 6 DIV (Figures S3B–S3L). The ability of Activin to upregulate expression of eye field markers (*Otx2*, *Six3*, *Rax*, *Six6*, *Vsx2*, *Tbx3*) decreased at higher doses, consistent with a stronger inhibition of neural differentiation (Figure S3M), whereas transcription of the telencephalic markers *Foxg1* and *Emx2* was always repressed (Figure S3M). Activin delivery in the absence of Wnti caused a stronger upregulation of mesendoderm markers (Figure S3B) and a weaker upregulation of eye field markers (Figure S3M) in comparison with treatments with both Wnti and Activin, suggesting that Activin elicits eye field fates specifically in anterior neural progenitors, which form more efficiently when the Wnt/β-catenin pathway is inhibited (Bertacchi et al., 2015). The effects of Activin in the presence of both Wnti and BMPi were similar to those of treatments without BMPi (Figures S3B–S3M), indicating that endogenous BMP signaling does not hinder eye field specification in this system. Treatments with the Activin/Nodal inhibitor SB431542 did not affect expression of eye field or telencephalic markers (Figure S3N), in agreement with the very low endogenous activation of Activin/Nodal signaling in these conditions (Bertacchi et al., 2015). Although these data suggest that Activin can steer pluripotent stem cells differentiating to anterior neuroectoderm toward eye field fates, their interpretation is complicated by the fact that early Activin treatments, in line with previous studies (Lupo et al., 2014; Vallier et al., 2004), interfere with mESC neuralization.

Activin Promotes Eye Field Fates within a Specific Time Window during Differentiation of mESCs to Anterior Neural Progenitors

To distinguish an earlier role of Activin/Nodal signaling in opposing neuroectoderm differentiation from a later role in anterior neural patterning, we focused on a moderate dose of Activin (10 ng/ml), which is more permissive toward mESC neuralization compared to higher doses (Figures S2C and S3), but started the treatments at different time points during anterior neural differentiation. Cultures were treated with Wnti from 3 DIV with or without Activin, which was added starting at the same time point or with increasing delays of 12, 24, 36, or 48 hr (Figure 2A); the percentage of the total cell count that was positive for *Rax*-GFP or OCT4 was then analyzed at 8 DIV. Cultures treated with Wnti alone differentiated efficiently to neuroectoderm (as shown by very few OCT4-positive cells), but they were refractory to eye field specification (5% *Rax*-GFP-positive cells; Figures 2B and 2C). When Activin was added together with Wnti (3 DIV), it promoted eye field specification (26.9% of *Rax*-GFP-positive cells; Figures 2B and 2D) but delayed neuroectoderm differentiation (18.9% of OCT4-positive cells persisting at 8 DIV; Figures 2B and 2D). Delaying the start of Activin treatment by 12–36 hr after Wnti delivery (3.5–4.5 DIV; Figure 2A) nearly doubled the percentage of *Rax*-GFP-positive cells (up to 45.2% *Rax*-GFP-positive cells at 8 DIV; Figures 2B–2G) without delaying differentiation (3% OCT4-positive cells at 8 DIV following Activin treatment from 4 DIV; Figures 2B–2G). No induction of *Rax*-GFP-positive cells was observed when cultures were treated with Activin starting from 5 DIV (5.5% *Rax*-GFP-positive cells at 8 DIV; Figures 2B and 2H). qRT-PCR analyses confirmed that transcription of *Six3*, *Rax*, *Six6*, and *Vsx2* peaked when Activin treatments were started between 12 and 36 hr after Wnti delivery (Figure 2I) but was similar to control (Wnt inhibition alone) levels when applying Activin 48 hr after Wnti (Figure 2I).

Activin treatment conditions causing optimal upregulation of eye field genes were also more effective at downregulating expression of telencephalic markers (Figure 2I). Activin efficiently enhanced eye field gene expression only in cultures treated with Wnti (Figures 2B and 2I), supporting the idea that Activin promotes eye field fates in anterior neural progenitors.

Higher Activin doses (50 ng/ml), even when delivered at 3.5 DIV (Figure S4A), decreased the fraction of *Rax*-GFP-positive cells at 8 DIV, probably due to maintenance of *Oct4* expression and delayed neuroectoderm differentiation (Figures S4B–S4M). Altogether, these results suggest that Activin plays different roles at different stages of mESC differentiation. At early stages (up to 3 DIV), Activin opposes neuroectoderm specification by promoting expression of pluripotency and mesendoderm genes. In

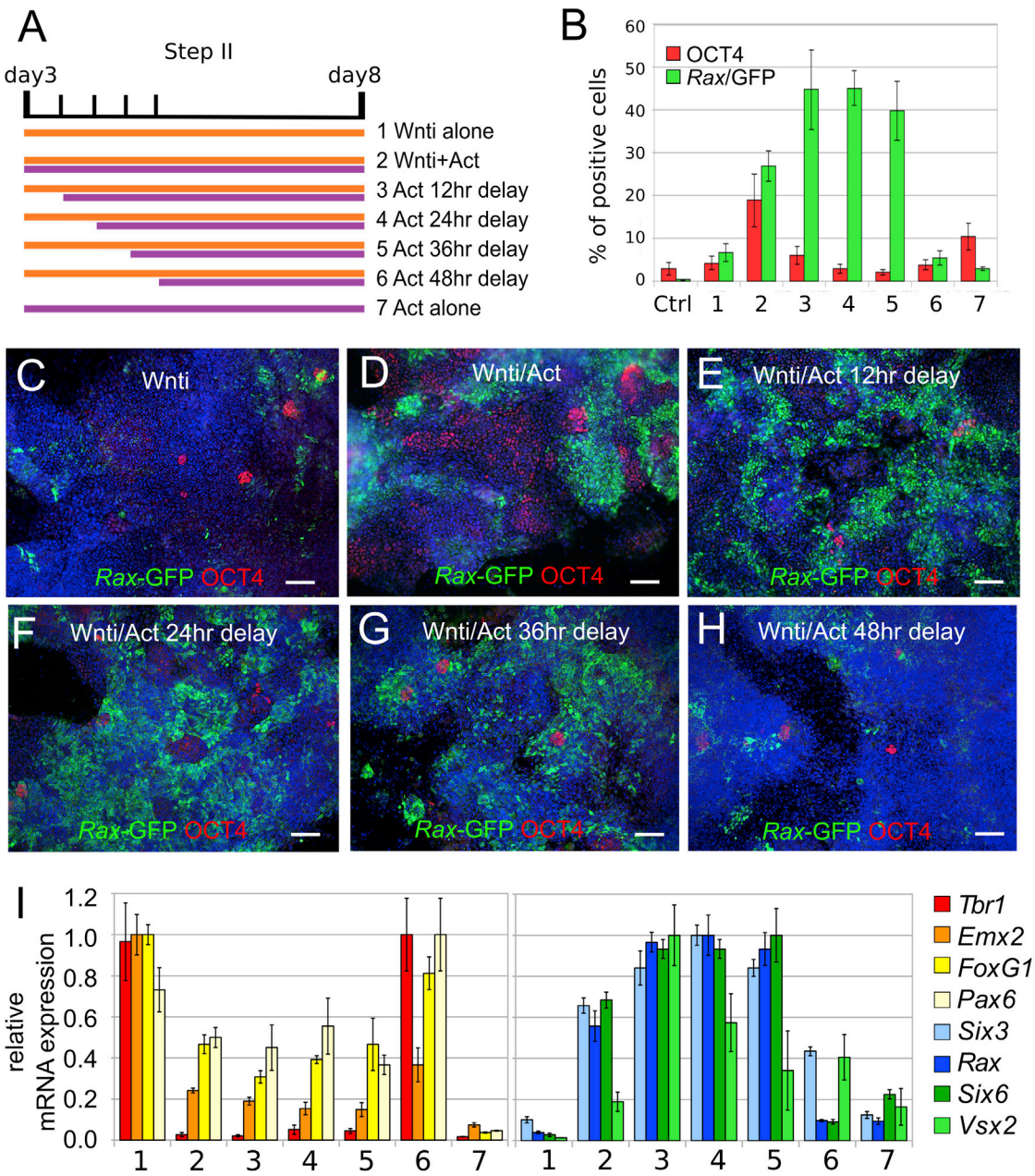

Figure 2. Activin Promotes *Rax* Expression within a Restricted Time Window during mESC Differentiation to Anterior Neuroectoderm

(A) Scheme of temporally controlled Activin treatments.

(B) Percentage of the total K/l EB5 cell count that was positive for OCT4 or *Rax*-GFP. Culture conditions were as in (A). Ctrl, control (CDMM). Error bars represent SEM (n = 3 independent experiments).

(C–H) Representative images of K/l EB5 cells differentiated in the conditions indicated in (A) and immunostained for both GFP and OCT4 at 8 DIV. The scale bars represent 50 μm.

(I) qRT-PCR of neuroectoderm (*Pax6*), telencephalic (*Tbr1*, *Emx2*, *FoxG1*), and eye field (*Six3*, *Rax*, *Six6*, *Vsx2*) gene expression in the conditions indicated in (A). Values are normalized to samples with maximal expression levels. Error bars were obtained from the error propagation formula (n = 3 independent experiments were pooled together; each experiment contained n = 2 technical replicates).

See also Figures S3 and S4.

early anterior neural progenitors, which emerge at 3.5–4.5 DIV in conditions of low Wnt signaling, moderate Activin levels promote eye field fates.

Activin Promotes Formation of *Rax*-Expressing Progenitors Bearing Retinal-Specific Regional Identities

In mouse embryos, strong *Rax* expression is found both in the developing retina and ventral hypothalamus (Wataya et al., 2008). Retinal progenitors express *Rax* and *Pax6*, whereas ventral hypothalamic progenitors express *Rax* and *Nkx2.1* (Ikeda et al., 2005; Wilson and Houart, 2004). Because Wnt inhibition and Activin/Nodal signaling have been implicated in hypothalamic development (Kapsimali et al., 2004; Mathieu et al., 2002), we investigated whether *Rax*-expressing progenitors generated in the presence of Wnti and Activin acquired retinal and/or hypothalamic identities. Sonic Hedgehog (SHH) signaling has a well-established role in promoting hypothalamic development (Ikeda et al., 2005; Wataya et al., 2008). Therefore, to better distinguish *Rax*-positive retinal fates from *Rax*-positive hypothalamic fates, we compared the identity of *Rax*-expressing progenitors forming in Activin-treated cultures with that of *Rax*-positive cells generated in cultures treated with SHH pathway agonists.

Rax-GFP-positive progenitors induced by treating differentiating mESC cultures with both Wnti (from 3 DIV) and Activin (from 3.5 DIV) were mostly PAX6 positive and NKX2.1 negative at 8 DIV (up to 40.7% *Rax*-GFP-positive cells, 32.4% *Rax*-GFP/PAX6 double-positive cells, 2.2% *Rax*-GFP/NKX2.1 double-positive cells; Figure 3), suggesting that they had acquired a retinal identity.

Previous studies indicated that activation of SHH signaling in mESCs differentiating to anterior neuroectoderm led to the specification of ventral hypothalamic progenitors expressing *Rax* and *Nkx2.1* (Wataya et al., 2008). To further confirm that *Rax*-positive cells generated in Activin-treated cultures acquired a retinal, rather than hypothalamic, identity, we generated *Rax*-positive ventral forebrain progenitors by means of treatments with a Smoothened agonist (SAG; 100 nM). SAG was added to differentiating mESC cultures from 3 DIV with or without Wnti. Some of these cultures were also treated with Activin from 3.5 DIV (Figure 3A). SAG robustly increased the percentage of *Rax*-GFP-positive cells (up to 61.6% of the total cell count) at 8 DIV, but only in cultures treated with Wnti (Figures 3B–3D). In contrast to Activin treatments, however, the vast majority of these cells were PAX6 negative and NKX2.1 positive (0.6% *Rax*-GFP/PAX6 double-positive cells, 60% *Rax*-GFP/NKX2.1 double-positive cells; Figures 3B and 3D), indicating acquisition of a ventral hypothalamic identity. NKX2.1-expressing cells were increased by SAG also in the absence of Wnti (65.3% NKX2.1-positive cells), but they were mostly *Rax*-GFP negative (Figures 3B and 3C). Activin and SAG treatments together did not show collaborative effects in the generation of *Rax*-GFP-positive cells, which were mostly PAX6 negative and NKX2.1 positive (Figures 3B–3D). Similar results were obtained when cultures were treated with Activin and different doses of SAG (1, 10, 100 nM; Figures S5A–S5D). Inhibition of SHH signaling with cyclopamine (5 μM) in cultures treated with Activin did not enhance either the generation of *Rax*-GFP-positive cells or the fraction of cells coexpressing *Rax*-GFP and PAX6 (Figures 3B–3D), in agreement with the observation that endogenous SHH signaling is inactive during the early stages of our differentiation protocol (Bertacchi et al., 2015).

Treatments with Wnti and Activin could promote formation of *Rax*-GFP/PAX6-positive (NKX2.1-negative) retinal progenitors even when cells were maintained as floating aggregates until harvesting at 10 DIV (Figures S5E and S5F). Treatments of floating aggregate cultures with Wnti and SAG led to formation of *Rax*-GFP/NKX2.1-positive (PAX6-negative) progenitors. Retinal progenitors were mainly present within superficial layers of Activin-treated cell aggregates, whereas hypothalamic progenitors could be found throughout SAG-treated aggregates. This may be explained by more limited diffusion of exogenous signaling proteins (as compared to small molecules) within cell aggregates.

We further characterized the positional identity of adherent cultures treated with either Wnti and Activin or Wnti and SAG by global transcriptomic analyses. We sorted *Rax*-positive (*Rax*$^+$) or *Rax*-negative (*Rax*$^-$) cells from these cultures at 10 DIV (Figures S6A–S6E) and used them, along with unsorted cells from cultures treated only with Wnti, for microarray-based comparative gene expression profiling with respect to eye, cortex, or hypothalamus/diencephalon explanted from embryonic day 12.5 mouse embryos (Figure 4; Figures S6F–S6H). Pearson correlation analysis indicated that cell cultures and embryonic tissues clustered separately, with high values of correlation among samples of the same category (Figure S6F). Principal component analysis (PCA) confirmed that cultures and tissues formed well-separated groups (Figure S6G). Moreover, it indicated that the large majority of genes whose expression varies among different samples (principal component 1, accounting for 92.7% of variance) is actually not separating them and that only a small ratio of gene expression variance (principal component 2, accounting for 2.2% of variance) is responsible for the difference between cell-culture sample and tissue sample groups (Figure S6G). These analyses suggested that the genes whose expression accounts for differences among different brain regions, and different cell-culture conditions, are few, and that the

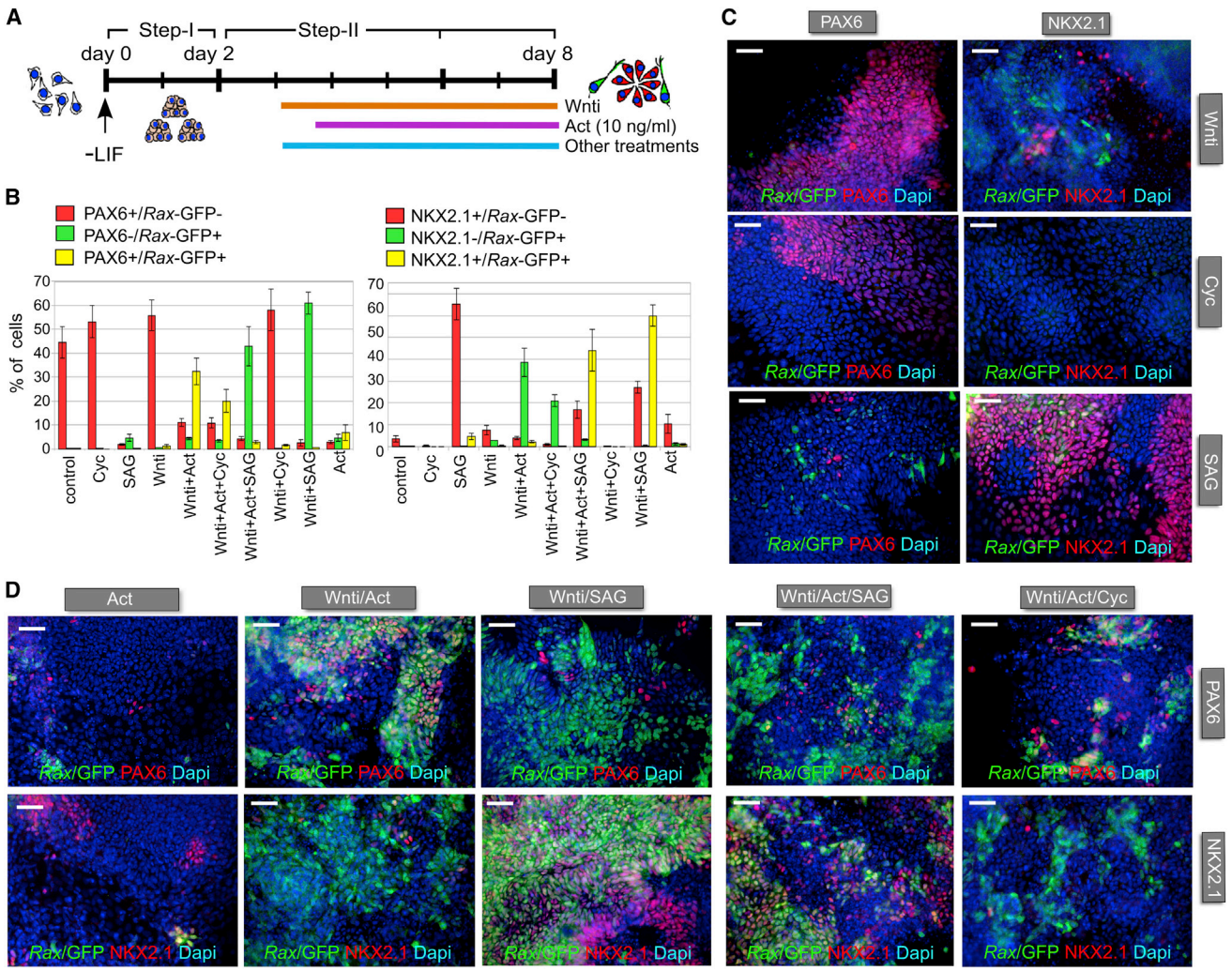

Figure 3. Activin and SHH Signaling Promote Retinal Progenitor or Ventral Forebrain Progenitor Identity, Respectively, in mESCs Differentiating to Anterior Neuroectoderm

(A) Scheme of anterior neural differentiation of mESCs in the presence of different signaling molecules. Activin was applied 12 hr after the start of Wnti treatments, whereas SAG or cyclopamine (Cyc) was delivered simultaneously with Wnti.

(B) Quantification of the percentage of the total K/l EB5 cell count that was positive for *Rax*-GFP and/or PAX6 (left chart) or for *Rax*-GFP and/or NKX2.1 (right chart), as detected by immunodetection at 8 DIV, following differentiation in the indicated conditions. Error bars represent SEM (n = 3 independent experiments).

(C and D) Representative images of K/l EB5 cells differentiated in the indicated conditions at 8 DIV. The scale bars represent 30 μm. See also Figure S5.

variance of their expression is masked by the variance of the rest of the genes. We then performed clustering and PCA on a transcriptome subset, including genes with highest variance among tissues or cultures (see the Experimental Procedures). Analysis of this subset indicated that cells treated with Wnti and Activin clustered with embryonic eye tissue and cells treated with Wnti and SAG clustered with embryonic hypothalamus/diencephalon, whereas control cultures treated with Wnti only clustered with embryonic cortex (Figures 4A and 4B). Notably, the values of correlation among samples of the same category (cell culture or tissue) were quite low, indicating that this subset of genes can discriminate different positional identities in both cell culture and tissue samples, regardless of their in vitro or in vivo origin (Figure 4A). Accordingly, the first two principal components of the PCA, together accounting for 49.8% and 19.3% of variance, respectively, divided the samples into the same three major clusters (corresponding to eye, hypothalamus/diencephalon, and cortex identities) identified by Pearson correlation analysis

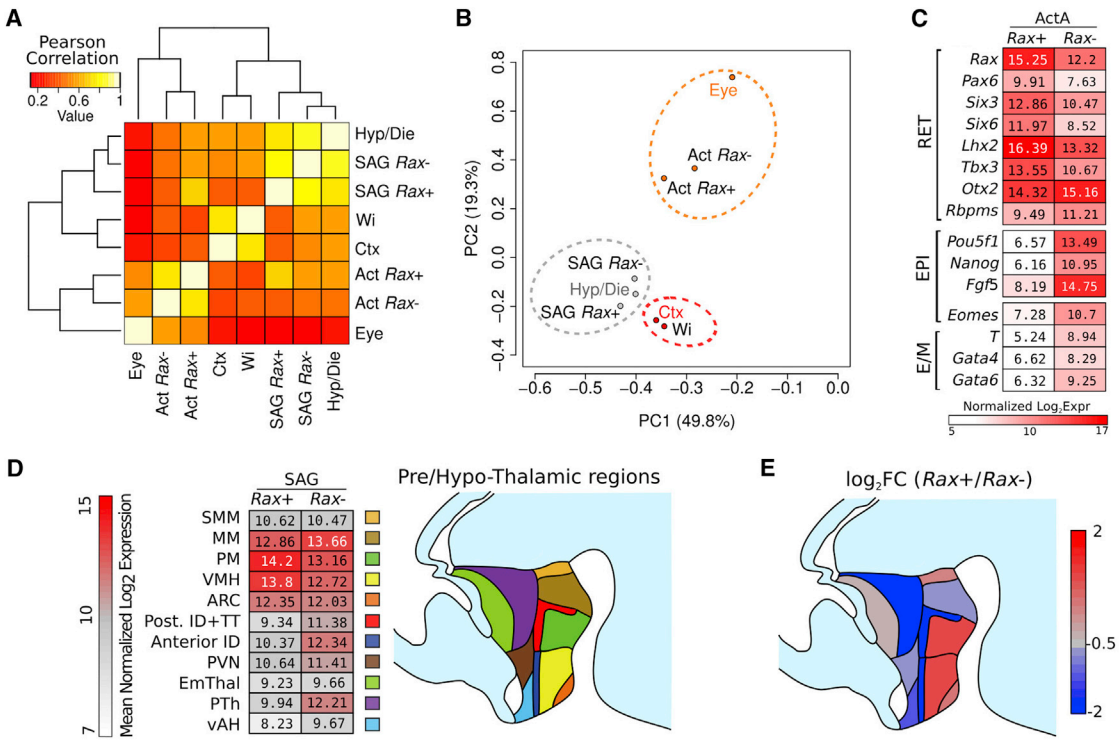

Figure 4. Cultures Treated with Activin or SAG Display Eye or Hypothalamic/Diencephalic Gene Expression Profiles, Respectively

(A) Clustering analysis, showing the distribution of Pearson correlation among transcriptome subsets of different cell cultures and embryonic brain regions. The subset of transcriptome analyzed consists of the 414 gene with the highest variance among cell cultures or tissues (top 2%; see the Experimental Procedures). Hyp/Die, hypothalamus/diencephalon; SAG, SHH agonist; *Rax*$^{+}$ and *Rax*$^{-}$, K/l EB5 cells positive or negative for GFP expression, respectively; Wi, Wnt inhibition; Ctx, cortex; Act, Activin.

(B) PCA of samples as in (A). PC1 and PC2 indicate the first and second principal component, respectively, with percentages of explained variance in parentheses.

(C) Color heatmap showing $\log_2$ mean normalized expression of selected gene subsets, marking retina (RET), epiblast (EPI), or endomesoderm (E/M) cell identity in Activin-treated *Rax*$^{+}$ and *Rax*$^{-}$ cells.

(D) Color heatmap showing $\log_2$ mean normalized expression of selected gene subsets in SAG-treated *Rax*$^{+}$ and *Rax*$^{-}$ cells. Each gene subset marks a specific prethalamic (purple and dark brown) or hypothalamic (other colors) region, as described in Shimogori et al. (2010).

(E) Color heatmap showing the $\log_2$ fold change (FC) ratio of the mean normalized expression values in (D). SMM, supramamillary nucleus; MM, mamillary nucleus; PM, premamillary region; VMH, ventromedial hypothalamic nucleus; ARC arcuate nucleus; ID, intrahypothalamic diagonal region; TT, tuberomamillary terminal region; PVN, paraventricular nucleus; EmThal, eminentia thalami; PTh, prethalamus; vAH, ventral anterior hypothalamus. Tissue samples were obtained from n = 3 embryos (wild-type, Sv129s6 mouse strain, Taconic) and pooled together before RNA extraction. In vitro samples were produced with n = 3 technical replicates; cells were dissociated and pooled together before processing.

See also Figure S6.

(Figure 4B). Unexpectedly, neither analysis was able to neatly separate *Rax*$^{+}$ from *Rax*$^{-}$ cells in cultures treated with Activin or SAG. A closer inspection of each transcriptome contributed to explaining why *Rax*$^{+}$ and *Rax*$^{-}$ cells seemed more homogeneous than expected when compared to embryonic tissues. In cultures treated with Activin, *Rax*$^{-}$ cells expressed higher levels of both epiblast and endo/mesoderm markers in comparison to *Rax*$^{+}$ cells but also appreciable levels of retinal markers, including *Rax*. This suggests that a fraction of these cells had activated *Rax* expression and started retinal differentiation, even if they had not yet accumulated enough GFP fluorescence, and that the ratio of GFP-positive cells at DIV 10 represents an underestimation of the fraction of cells with a retinal gene expression profile. In cultures treated with SAG, both *Rax*$^{+}$ and *Rax*$^{-}$ cells expressed a substantial number of hypothalamic and prethalamic markers (Figure 4C and data not shown). We then extrapolated small subsets of markers that identify distinct hypothalamic and/or prethalamic regions, as previously described (Shimogori et al., 2010; Figure 4C; Figure S6H). This analysis indicated that *Rax*$^{+}$ cells preferentially express markers of ventral

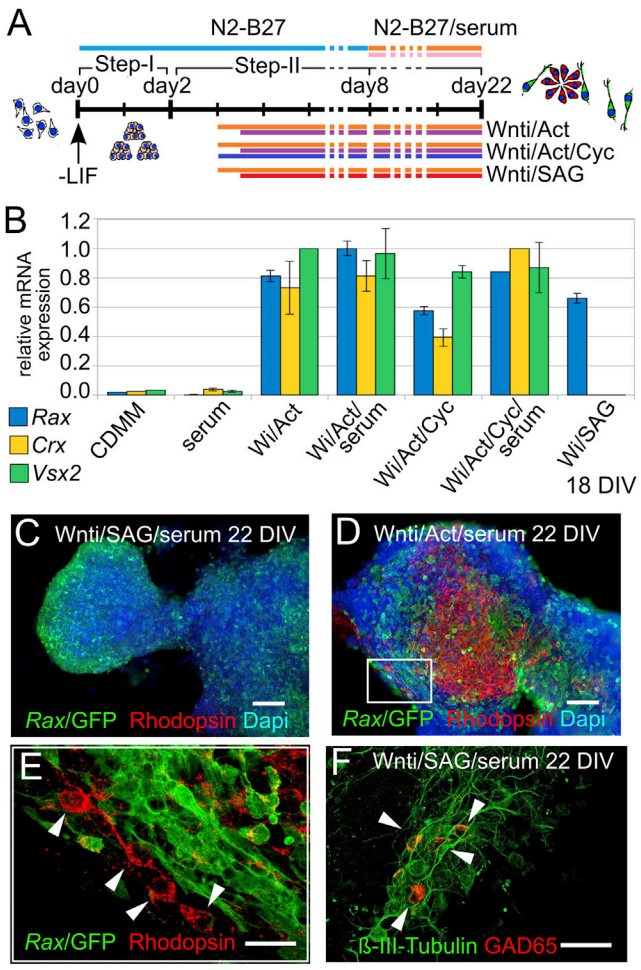

Figure 5. Terminal Differentiation of Activin-Treated Cells or SAG-Treated Cells Generates Rhodopsin-Positive Neurons or Gad65-Positive Neurons, Respectively

(A) Scheme of long-term mESC differentiation in the presence of Wnti and Activin (Wnti/Act), with or without Cyc, or with Wnti and SAG (Wnti/SAG). Activin and SAG were applied 12 hr after the start of Wnti treatments, whereas Cyc was delivered simultaneously with Wnti.

(B) qRT-PCR of retinal marker (*Rax*, *Crx*, *Vsx2*) expression 18 DIV. Results are normalized to samples with maximal expression levels for each marker. Error bars were obtained from the error propagation formula (n = 3 independent experiments).

(C–F) Representative images of K/l EB5 cells differentiated in the indicated conditions at 22 DIV. Rhodopsin-positive cells are indicated by arrowheads in (E). Gad65-positive neurons (27.6% GAD65-positive cells among B-III-Tub-positive neurons) are indicated by arrowheads in (F). The boxed area in (D) is shown at higher magnification in (E). The scale bars represent 30 μm (C and D), 10 μm (E), and 15 μm (F).

See also Figure S7.

hypothalamic regions, whereas *Rax*$^{-}$ cells tend to express markers of more dorsal hypothalamic regions or prethalamic areas (Figure 4D), in agreement with the distribution of *Rax* expression in the developing hypothalamus and diencephalon (Wataya et al., 2008).

Our results suggest that both Activin and SHH signaling are able to drive *Rax* expression in early anterior neural progenitors, but that they work independently of each other promoting alternative cell fates. Different from SHH signaling, Activin supports formation of retinal progenitors coexpressing *Rax* and PAX6, rather than *Rax*-NKX2.1-positive ventral hypothalamic progenitors. To further support these conclusions, we evaluated the ability of *Rax*$^{+}$ progenitors induced by Activin or SAG treatments to undertake a retinal neuron differentiation program in long-term cultures (up to 22 DIV; Figure 5A). Besides *Rax*, cells treated with Wnti and Activin (10 ng/ml, 12-hr delayed treatment), but not SAG, transcribed *Crx*, a marker of immature photoreceptor cells, *Vsx2*, a marker of differentiating bipolar cells, and *Brn3b*, a marker of differentiating retinal ganglion cells, at 18–22 DIV (Figure 5B; Figure S7F). At 22 DIV, cells positive for Rhodopsin, a marker of more mature photoreceptors, were evident in these cultures (Figures 5D and 5E) but not in control or SAG-treated cultures (data not shown). Rhodopsin-positive cells were preferentially located in close proximity to clusters of *Rax*-GFP-positive retinal progenitors, but they showed weak *Rax*-GFP signal themselves (Figures 5D and 5E). This is consistent with the fact that retinal progenitors switch off *Rax* expression when they undergo terminal differentiation (Furukawa et al., 1997a, 1997b). In contrast, SAG-treated long-term cultures produced GAD65-positive neurons (27.6%; Figure 5F). At 22 DIV, cells treated with both Wnti and Activin also upregulated other markers of retinal neuron differentiation in comparison with Wnti-treated samples. In addition to Rhodopsin, Cone Opsin (cones), BRN3 (ganglion cells), VSX2 (bipolar cells), and Recoverin (pan-photoreceptor) were detected in significant percentages of cells (Figures S7A–S7E and S7G). These results suggest that *Rax*-expressing progenitors generated in the presence of Activin mainly acquire a retinal identity, which can be distinguished from SHH-dependent hypothalamic fates.

Activin Promotes Eye Field Gene Expression in Differentiating hESCs

Culture of hESCs as floating aggregates in a chemically defined minimal medium (CDMM) (Vallier et al., 2004) is permissive, to some extent, for differentiation to neural progenitors expressing early anterior neural markers such as *OTX2* and *PAX6* (Patani et al., 2009; Smith et al., 2008; Vallier et al., 2004). We therefore used this straightforward experimental system to address whether Activin

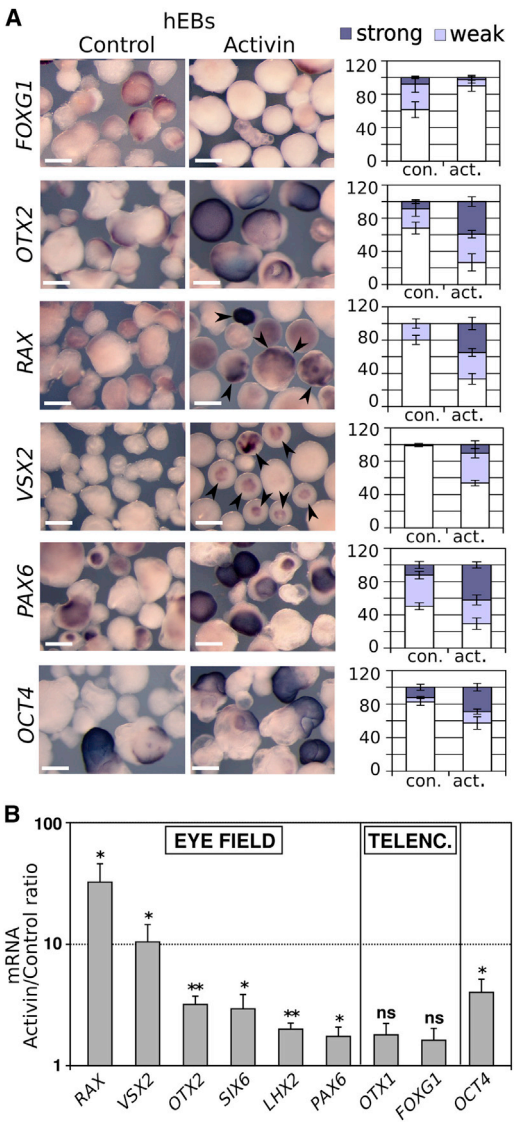

Figure 6. Activin Promotes Eye Field Gene Expression in Differentiating hESCs

(A) In situ hybridization on floating aggregates obtained following a 12-day differentiation of hESCs in nonadherent conditions either in plain CDMM or in the presence of Activin, as indicated. Arrowheads point to *RAX*-positive or *VSX2*-positive aggregates. Bar histograms show the percentage of aggregates displaying strong (dark purple), weak (light blue), or absent (white) signal. The scale bars represent 0.8 mm. Error bars represent SEM. (At least 100 aggregates for each culture condition and probe from one representative experiment were used for these analyses.) hEBs, human embryoid bodies.

(B) qRT-PCR of gene expression in hESCs differentiated as floating aggregates for 12–14 days with or without Activin. Results are shown as the mean ratio between Activin and control conditions. Error bars represent SEM. *$p < 0.05$; **$p < 0.01$; ns, nonsignificant ($p \geq 0.05$) according to Student's t test performed between Activin and control conditions ($n = 8$ independent experiments).

treatments could promote eye field gene expression in differentiating hESCs. hESCs were differentiated as floating aggregates for 12–14 days in basic CDMM or CDMM supplemented with 50 ng/ml Activin. These doses of Activin were chosen to compensate for limited diffusion of exogenous growth factors within hESC aggregates, as previously described (Vallier et al., 2004). Cell aggregates were then harvested for molecular marker analyses by in situ hybridization and qRT-PCR. As detected by in situ hybridization, Activin treatments increased the number of *OCT4*-positive aggregates, although the majority of the aggregates were *OCT4* negative (Figure 6A). Thus, Activin could delay, but not prevent, hESC differentiation in these conditions. Nonetheless, compared with controls, Activin-treated cultures showed stronger expression of eye field markers (*OTX2*, *RAX*, *VSX2*, *PAX6*), but not of the telencephalic marker *FOXG1*, both in terms of percentage of positive aggregates and staining intensity (Figure 6A). qRT-PCR analysis confirmed a significant increase in transcription levels of several eye field markers (*RAX*, *VSX2*, *SIX6*, *OTX2*, *LHX2*, *PAX6*) following Activin treatments, whereas telencephalic markers (*OTX1*, *FOXG1*) were not significantly affected (Figure 6B). These data suggest that Activin can support the expression of eye field genes during differentiation of both mESCs and hESCs.

DISCUSSION

The extracellular signals that induce the EFTF network in retinal progenitors are poorly understood. Although inhibition of BMP and Wnt/β-catenin signaling has been implicated in eye field formation (Cavodeassi et al., 2005; Lan et al., 2009), transient downregulation of these pathways appears to be a prerequisite for the initial specification of the entire secondary prosencephalon. How the telencephalon, eye field, and hypothalamus are then diversified within this prosencephalic tissue remains unclear.

In ESC in vitro systems, culture conditions devoid of exogenous signals or supplemented with inhibitors of endogenous signals were not sufficient for efficient generation of retinal progenitors and they drove instead hypothalamic or telencephalic specification (Bertacchi et al., 2015; Lupo et al., 2013; Nicoleau et al., 2013; Wataya et al., 2008). To date, efficient acquisition of retinal identity has been achieved via poorly defined exogenous cues, including complex extracellular matrices (ECMs) and biological supplements (Lupo et al., 2014; Viczian, 2013; Boucherie et al., 2013; Eiraku et al., 2011; Gonzalez-Cordero et al., 2013; Zhu et al., 2013)

Previous work suggested that Activin/Nodal signaling promotes eye field fates in ESCs. In particular, supplementation of serum and serum replacement media with Activin

increased the production of retinal progenitors from mESCs (Ikeda et al., 2005). Subsequently, a combination of the Nodal and ECM molecules entactin and laminin was found to mimic retinal progenitor induction by Matrigel (Eiraku et al., 2011). Finally, inhibitors of the Activin/Nodal pathway repressed eye field gene expression during neuroectoderm differentiation of hESCs (Lupo et al., 2013). These studies, however, did not clarify the role of Activin/Nodal signaling in retinal progenitor specification.

In this study, we show that Activin promotes eye field fates in mESCs differentiating to anterior neuroectoderm in chemically defined minimal media. Activin effectively upregulated eye field gene expression only when delivered at moderate doses and within a narrow 24-hr time window during early steps of neuroectoderm differentiation. In agreement with previous literature (Lupo et al., 2014; Smith et al., 2008; Vallier et al., 2004), treatments at higher doses and/or earlier time points promoted pluripotency and mesendoderm differentiation and repressed neuroectoderm differentiation, whereas later treatments could not support retinal identity. Moreover, Activin efficiently enhanced eye field specification only in cultures treated with inhibitors of Wnt/β-catenin signaling, which promote anterior neural fates at the expense of posterior fates in differentiating ESCs (Bertacchi et al., 2013; Lupo et al., 2013, 2014; Nicoleau et al., 2013). Hence, the effects of Activin are dependent on the competence of the responding cells: we speculate that Activin can upregulate eye field genes in primitive forebrain progenitors, but not in pluripotent cells, later forebrain progenitors, or posterior neural progenitors. We observed Activin-dependent upregulation of eye field genes in either adherent or floating aggregate cultures. Activin enhanced eye field gene expression also in hESCs differentiating as floating aggregates in chemically defined medium devoid of ECM components and serum replacement, indicating that the ability of Activin to promote eye field fates is not limited to mouse ESCs or to a specific cell line or culture method.

In mouse embryos, both the developing retina and the ventral hypothalamus show strong *Rax* expression (Ikeda et al., 2005; Wataya et al., 2008; Wilson and Houart, 2004). Consistent with previous studies (Ikeda et al., 2005; Wataya et al., 2008), we confirmed that SHH agonists upregulated *Rax* in mESCs but in the context of ventral hypothalamic specification, because *Rax*-expressing cells were positive for NKX2.1 and negative for PAX6. Upon terminal differentiation, these cultures generated GAD65-positive neurons. Side-by-side comparison of Activin and SAG treatments confirmed that the effects of these molecules were clearly distinguishable. Activin, but not SAG, supported specification of *Rax*-PAX6-positive retinal progenitors, which were endowed with transcriptomic profiles clustering with those of embryonic eye tissue and were capable of undertaking retinal neuron differentiation in long-term cultures.

Activin/Nodal signaling controls early vertebrate development at multiple levels, and it is difficult to distinguish direct roles in eye development from indirect effects. Forebrain and eye formation are affected in fish and mouse mutants with defective Activin/Nodal signaling (Lu and Robertson, 2004; Varlet et al., 1997; Wilson and Houart, 2004), but these effects are likely due to the disruption of mesendodermal signaling centers required for rostral neuroectoderm formation (Wilson and Houart, 2004). Excessive Activin/Nodal signaling, however, can repress anterior neural fates by maintaining pluripotency and/or promoting mesendoderm differentiation within the ectoderm (Thisse et al., 2000; Vallier et al., 2004). Anterior neural induction occurs prematurely in the epiblast of *Nodal* mouse mutants (Camus et al., 2006), but although telencephalic genes are upregulated in Nodal-deficient anterior neuroectoderm, eye field markers (*Six3* and *Pax6*) are not properly expressed (Camus et al., 2006). Furthermore, during eye morphogenesis, eye field cells migrating laterally to form the optic vesicles become exposed to Activin-like signals released by extraocular tissues. Although these signals are involved in retinal pigment epithelium and anterior eye segment specification (Fuhrmann et al., 2000; Ittner et al., 2005), they might also support retinal progenitor identity. Highlighting the complex functions of Activin/Nodal signaling in eye development, recent studies in *Xenopus* found opposite effects of Nodal signaling inhibition on the specification of retinal identity using different experimental assays (Messina et al., 2015; Wong et al., 2015). Clearly, the roles of Activin/Nodal signaling in eye formation are much more difficult to dissect in vivo than they are in vitro, and further investigations in animal model organisms are warranted.

The results described in this and previous studies using ESC in vitro systems (Bertacchi et al., 2013, 2015; Lupo et al., 2013, 2014) lead to a model of the role of the Activin/Nodal pathway in the specification of retinal identity (Figure 7). In this model, downregulation of Activin/Nodal signaling in pluripotent cells leads to the emergence of early anterior neural progenitors, which can acquire rostral forebrain fates (corresponding to progenitors of the secondary prosencephalon in vivo) or caudal forebrain fates (corresponding to progenitors of the diencephalic/mesencephalic regions in vivo) depending on the levels of Wnt/β-catenin signaling, as previously described (Lupo et al., 2014 and references therein). Without further signaling, primitive rostral forebrain progenitors spontaneously evolve toward a default cortical identity (Bertacchi et al., 2013; Lupo et al., 2014), whereas they can be steered to retinal fates under the influence of Activin. As in

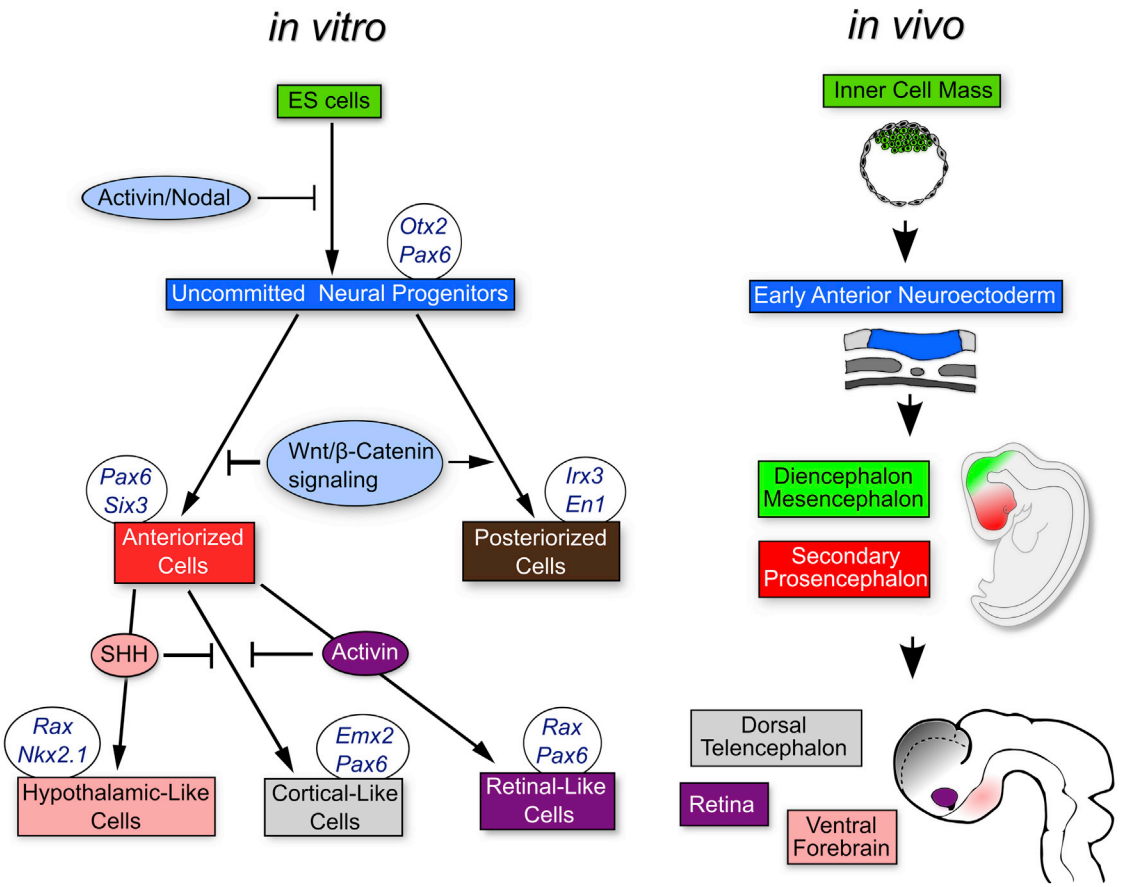

Figure 7. Model of the Roles of the Activin/Nodal, Wnt/β-Catenin, and SHH Signaling Pathways in the Induction of Rostral Forebrain Precursors

Embryonic structures and stages of mouse development in vivo corresponding to the progressively more fate-restricted progenitors emerging during ESC differentiation in vitro are shown. See text for details.

previous studies (Ikeda et al., 2005; Wataya et al., 2008), SHH signaling instead promotes ventral hypothalamic fates. Although more work is needed to address the function of Activin/Nodal signals during early eye development in vivo, this model provides a framework for future studies aimed at clarifying the mechanisms of eye field formation and producing retinal progenitors for basic research or therapy.

EXPERIMENTAL PROCEDURES

Murine ESC lines E14Tg2A (passages 25–38) and K/l EB5 (transgenic Rax-GFP ESCs, used with the kind permission of Y. Sasai, RIKEN Center) and H9 hESCs (WiCell) were cultured as described (Bertacchi et al., 2013; Lupo et al., 2013). All animal protocols were reviewed and approved by the Animal Protocol Review Committee at ITB-CNR of Pisa.

Detailed experimental procedures are available in Supplemental Information.

ACCESSION NUMBERS

The accession number for the microarray gene expression data reported in this paper is GEO: GSE71830.

SUPPLEMENTAL INFORMATION

Supplemental Information includes Supplemental Experimental Procedures and seven figures and can be found with this article online at http://dx.doi.org/10.1016/j.stemcr.2015.08.011.

ACKNOWLEDGMENTS

We are grateful to Morgan Alexander for help with hESC culture. We thank Kawssar Harb and Joséphine Parisot for their kind help with confocal imaging, and Elena Chiavacci for her hints about in situ hybridization. This work was supported by the Biotechnology and Biological Sciences Research Council (W.A.H., G.L.), Wellcome Trust (W.A.H.), Italian Ministry of Education, University and Research programme "Rientro dei Cervelli" and a start-up grant from Istituto Pasteur-Fondazione Cenci Bolognetti (G.L.),

Medical Research Council (R.A.P.), Flagship Project InterOmics PB.05, and Italian Ministry of Education, University and Research grant PRIN-2102 (F.C.).

Received: March 19, 2015
Revised: August 21, 2015
Accepted: August 21, 2015
Published: September 17, 2015

REFERENCES

Andoniadou, C.L., and Martinez-Barbera, J.P. (2013). Developmental mechanisms directing early anterior forebrain specification in vertebrates. Cell. Mol. Life Sci. *70*, 3739–3752.

Bertacchi, M., Pandolfini, L., Murenu, E., Viegi, A., Capsoni, S., Cellerino, A., Messina, A., Casarosa, S., and Cremisi, F. (2013). The positional identity of mouse ES cell-generated neurons is affected by BMP signaling. Cell. Mol. Life Sci. *70*, 1095–1111.

Bertacchi, M., Pandolfini, L., D'Onofrio, M., Brandi, R., and Cremisi, F. (2015). The double inhibition of endogenously produced BMP and Wnt factors synergistically triggers dorsal telencephalic differentiation of mouse ES cells. Dev. Neurobiol. *75*, 66–79.

Besser, D. (2004). Expression of Nodal, Lefty-A, and Lefty-B in undifferentiated human embryonic stem cells requires activation of Smad2/3. J. Biol. Chem. *279*, 45076–45084.

Boucherie, C., Mukherjee, S., Henckaerts, E., Thrasher, A.J., Sowden, J.C., and Ali, R.R. (2013). Brief report: self-organizing neuroepithelium from human pluripotent stem cells facilitates derivation of photoreceptors. Stem Cells *31*, 408–414.

Camus, A., Perea-Gomez, A., Moreau, A., and Collignon, J. (2006). Absence of Nodal signaling promotes precocious neural differentiation in the mouse embryo. Dev. Biol. *295*, 743–755.

Cavodeassi, F., Carreira-Barbosa, F., Young, R.M., Concha, M.L., Allende, M.L., Houart, C., Tada, M., and Wilson, S.W. (2005). Early stages of zebrafish eye formation require the coordinated activity of Wnt11, Fz5, and the Wnt/beta-catenin pathway. Neuron *47*, 43–56.

Eiraku, M., Takata, N., Ishibashi, H., Kawada, M., Sakakura, E., Okuda, S., Sekiguchi, K., Adachi, T., and Sasai, Y. (2011). Self-organizing optic-cup morphogenesis in three-dimensional culture. Nature *472*, 51–56.

Fuhrmann, S., Levine, E.M., and Reh, T.A. (2000). Extraocular mesenchyme patterns the optic vesicle during early eye development in the embryonic chick. Development *127*, 4599–4609.

Furukawa, T., Kozak, C.A., and Cepko, C.L. (1997a). rax, a novel paired-type homeobox gene, shows expression in the anterior neural fold and developing retina. Proc. Natl. Acad. Sci. USA *94*, 3088–3093.

Furukawa, T., Morrow, E.M., and Cepko, C.L. (1997b). Crx, a novel otx-like homeobox gene, shows photoreceptor-specific expression and regulates photoreceptor differentiation. Cell *91*, 531–541.

Gonzalez-Cordero, A., West, E.L., Pearson, R.A., Duran, Y., Carvalho, L.S., Chu, C.J., Naeem, A., Blackford, S.J.I., Georgiadis, A., Lakowski, J., et al. (2013). Photoreceptor precursors derived from three-dimensional embryonic stem cell cultures integrate and mature within adult degenerate retina. Nat. Biotechnol. *31*, 741–747.

Hemmati-Brivanlou, A., Kelly, O.G., and Melton, D.A. (1994). Follistatin, an antagonist of activin, is expressed in the Spemann organizer and displays direct neuralizing activity. Cell *77*, 283–295.

Ikeda, H., Osakada, F., Watanabe, K., Mizuseki, K., Haraguchi, T., Miyoshi, H., Kamiya, D., Honda, Y., Sasai, N., Yoshimura, N., et al. (2005). Generation of Rx+/Pax6+ neural retinal precursors from embryonic stem cells. Proc. Natl. Acad. Sci. USA *102*, 11331–11336.

Ittner, L.M., Wurdak, H., Schwerdtfeger, K., Kunz, T., Ille, F., Leveen, P., Hjalt, T.A., Suter, U., Karlsson, S., Hafezi, F., et al. (2005). Compound developmental eye disorders following inactivation of TGFbeta signaling in neural-crest stem cells. J. Biol. *4*, 11.

Kapsimali, M., Caneparo, L., Houart, C., and Wilson, S.W. (2004). Inhibition of Wnt/Axin/beta-catenin pathway activity promotes ventral CNS midline tissue to adopt hypothalamic rather than floorplate identity. Development *131*, 5923–5933.

Kim, S.W., Yoon, S.-J., Chuong, E., Oyolu, C., Wills, A.E., Gupta, R., and Baker, J. (2011). Chromatin and transcriptional signatures for Nodal signaling during endoderm formation in hESCs. Dev. Biol. *357*, 492–504.

Lan, L., Vitobello, A., Bertacchi, M., Cremisi, F., Vignali, R., Andreazzoli, M., Demontis, G.C., Barsacchi, G., and Casarosa, S. (2009). Noggin elicits retinal fate in *Xenopus* animal cap embryonic stem cells. Stem Cells *27*, 2146–2152.

Lu, C.C., and Robertson, E.J. (2004). Multiple roles for Nodal in the epiblast of the mouse embryo in the establishment of anterior-posterior patterning. Dev. Biol. *273*, 149–159.

Lupo, G., Novorol, C., Smith, J.R., Vallier, L., Miranda, E., Alexander, M., Biagioni, S., Pedersen, R.A., and Harris, W.A. (2013). Multiple roles of Activin/Nodal, bone morphogenetic protein, fibroblast growth factor and Wnt/β-catenin signalling in the anterior neural patterning of adherent human embryonic stem cell cultures. Open Biol. *3*, 120167.

Lupo, G., Bertacchi, M., Carucci, N., Augusti-Tocco, G., Biagioni, S., and Cremisi, F. (2014). From pluripotency to forebrain patterning: an in vitro journey astride embryonic stem cells. Cell. Mol. Life Sci. *71*, 2917–2930.

Mathieu, J., Barth, A., Rosa, F.M., Wilson, S.W., and Peyriéras, N. (2002). Distinct and cooperative roles for Nodal and Hedgehog signals during hypothalamic development. Development *129*, 3055–3065.

Meno, C., Gritsman, K., Ohishi, S., Ohfuji, Y., Heckscher, E., Mochida, K., Shimono, A., Kondoh, H., Talbot, W.S., Robertson, E.J., et al. (1999). Mouse Lefty2 and zebrafish antivin are feedback inhibitors of nodal signaling during vertebrate gastrulation. Mol. Cell *4*, 287–298.

Messina, A., Lan, L., Incitti, T., Bozza, A., Andreazzoli, M., Vignali, R., Cremisi, F., Bozzi, Y., and Casarosa, S. (2015). Noggin-mediated retinal induction reveals a novel interplay between bone morphogenetic protein inhibition, transforming growth factor β, and Sonic Hedgehog signaling. Stem Cells *33*, 2496–2508.

Mullen, A.C., Orlando, D.A., Newman, J.J., Lovén, J., Kumar, R.M., Bilodeau, S., Reddy, J., Guenther, M.G., DeKoter, R.P., Young, R.A.,

et al. (2011). Chromatin and transcriptional signatures for Nodal signaling during endoderm formation in hESCs. Cell *147*, 492–504.

Nicoleau, C., Varela, C., Bonnefond, C., Maury, Y., Bugi, A., Aubry, L., Viegas, P., Bourgois-Rocha, F., Peschanski, M., and Perrier, A.L. (2013). Embryonic stem cells neural differentiation qualifies the role of Wnt/β-catenin signals in human telencephalic specification and regionalization. Stem Cells *31*, 1763–1774.

Patani, R., Compston, A., Puddifoot, C.A., Wyllie, D.J.A., Hardingham, G.E., Allen, N.D., and Chandran, S. (2009). Activin/Nodal inhibition alone accelerates highly efficient neural conversion from human embryonic stem cells and imposes a caudal positional identity. PLoS ONE *4*, e7327.

Perea-Gomez, A., Vella, F.D.J., Shawlot, W., Oulad-Abdelghani, M., Chazaud, C., Meno, C., Pfister, V., Chen, L., Robertson, E., Hamada, H., et al. (2002). Nodal antagonists in the anterior visceral endoderm prevent the formation of multiple primitive streaks. Dev. Cell *3*, 745–756.

Shimogori, T., Lee, D.A., Miranda-Angulo, A., Yang, Y., Wang, H., Jiang, L., Yoshida, A.C., Kataoka, A., Mashiko, H., Avetisyan, M., et al. (2010). A genomic atlas of mouse hypothalamic development. Nat. Neurosci. *13*, 767–775.

Smith, J.R., Vallier, L., Lupo, G., Alexander, M., Harris, W.A., and Pedersen, R.A. (2008). Inhibition of Activin/Nodal signaling promotes specification of human embryonic stem cells into neuroectoderm. Dev. Biol. *313*, 107–117.

Thisse, B., Wright, C.V., and Thisse, C. (2000). Activin- and Nodal-related factors control antero-posterior patterning of the zebrafish embryo. Nature *403*, 425–428.

Vallier, L., Reynolds, D., and Pedersen, R.A. (2004). Nodal inhibits differentiation of human embryonic stem cells along the neuroectodermal default pathway. Dev. Biol. *275*, 403–421.

Varlet, I., Collignon, J., and Robertson, E.J. (1997). nodal expression in the primitive endoderm is required for specification of the anterior axis during mouse gastrulation. Development *124*, 1033–1044.

Viczian, A.S. (2013). Advances in retinal stem cell biology. J. Ophthalmic Vis. Res. *8*, 147–159.

Wataya, T., Ando, S., Muguruma, K., Ikeda, H., Watanabe, K., Eiraku, M., Kawada, M., Takahashi, J., Hashimoto, N., and Sasai, Y. (2008). Minimization of exogenous signals in ES cell culture induces rostral hypothalamic differentiation. Proc. Natl. Acad. Sci. USA *105*, 11796–11801.

Wilson, S.W., and Houart, C. (2004). Early steps in the development of the forebrain. Dev. Cell *6*, 167–181.

Wong, K.A., Trembley, M., Abd Wahab, S., and Viczian, A.S. (2015). Efficient retina formation requires suppression of both Activin and BMP signaling pathways in pluripotent cells. Biol. Open *4*, 573–583.

Yamamoto, M., Meno, C., Sakai, Y., Shiratori, H., Mochida, K., Ikawa, Y., Saijoh, Y., and Hamada, H. (2001). The transcription factor FoxH1 (FAST) mediates Nodal signaling during anterior-posterior patterning and node formation in the mouse. Genes Dev. *15*, 1242–1256.

Zhou, J., Su, P., Li, D., Tsang, S., Duan, E., and Wang, F. (2010). High-efficiency induction of neural conversion in human ESCs and human induced pluripotent stem cells with a single chemical inhibitor of transforming growth factor beta superfamily receptors. Stem Cells *28*, 1741–1750.

Zhu, Y., Carido, M., Meinhardt, A., Kurth, T., Karl, M.O., Ader, M., and Tanaka, E.M. (2013). Three-dimensional neuroepithelial culture from human embryonic stem cells and its use for quantitative conversion to retinal pigment epithelium. PLoS ONE *8*, e54552.

Stem Cell Reports

Supplemental Information

Activin/Nodal Signaling Supports Retinal Progenitor Specification in a Narrow Time Window during Pluripotent Stem Cell Neuralization

Michele Bertacchi, Giuseppe Lupo, Luca Pandolfini, Simona Casarosa, Mara D'Onofrio, Roger A. Pedersen, William A. Harris, and Federico Cremisi

SUPPLEMENTAL FIGURES

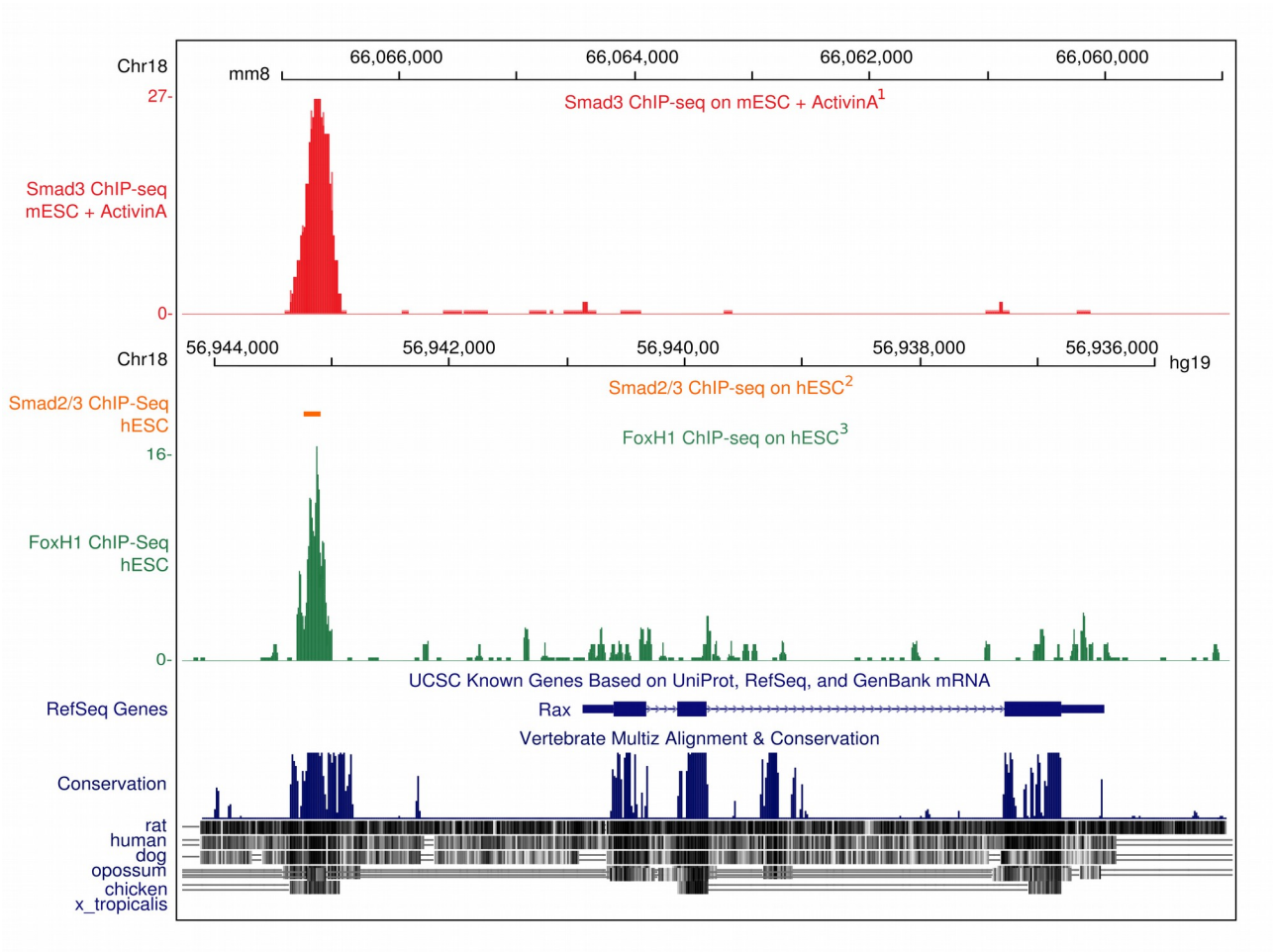

Figure S1, Related to Figure 1. SMAD2/3 and FOXH1 binding upstream of *Rax* promoter region in mouse and human ESCs. (A) Gene plots showing density of mouse SMAD3 (red; 1: GSM539542; Mullen et al., 2011), human SMAD2/3 (orange; 2: GSM727557; Kim et al., 2011) and human FOXH1 (green; 3: GSM727564; Kim et al., 2011) at *Rax* gene in mouse or human ESCs. Orange bar indicates the only region with a significant density of SMAD2/3 association. Values on the Y axis indicate reads per million (see Supplemental Experimental Procedures). Genomic positions reflect NCBI mouse genome build 36 (mm8) and human genomic buid 37 (hg19). Vertebrate Multiz Alignment & Conservation (UCSC Genome Browser; Kent et al., 2002) shows the evolutionary conservation of *Rax* exons and putative promoter region, including SMAD2/3 and FOXH1 binding site (blue peaks) among vertebrates.

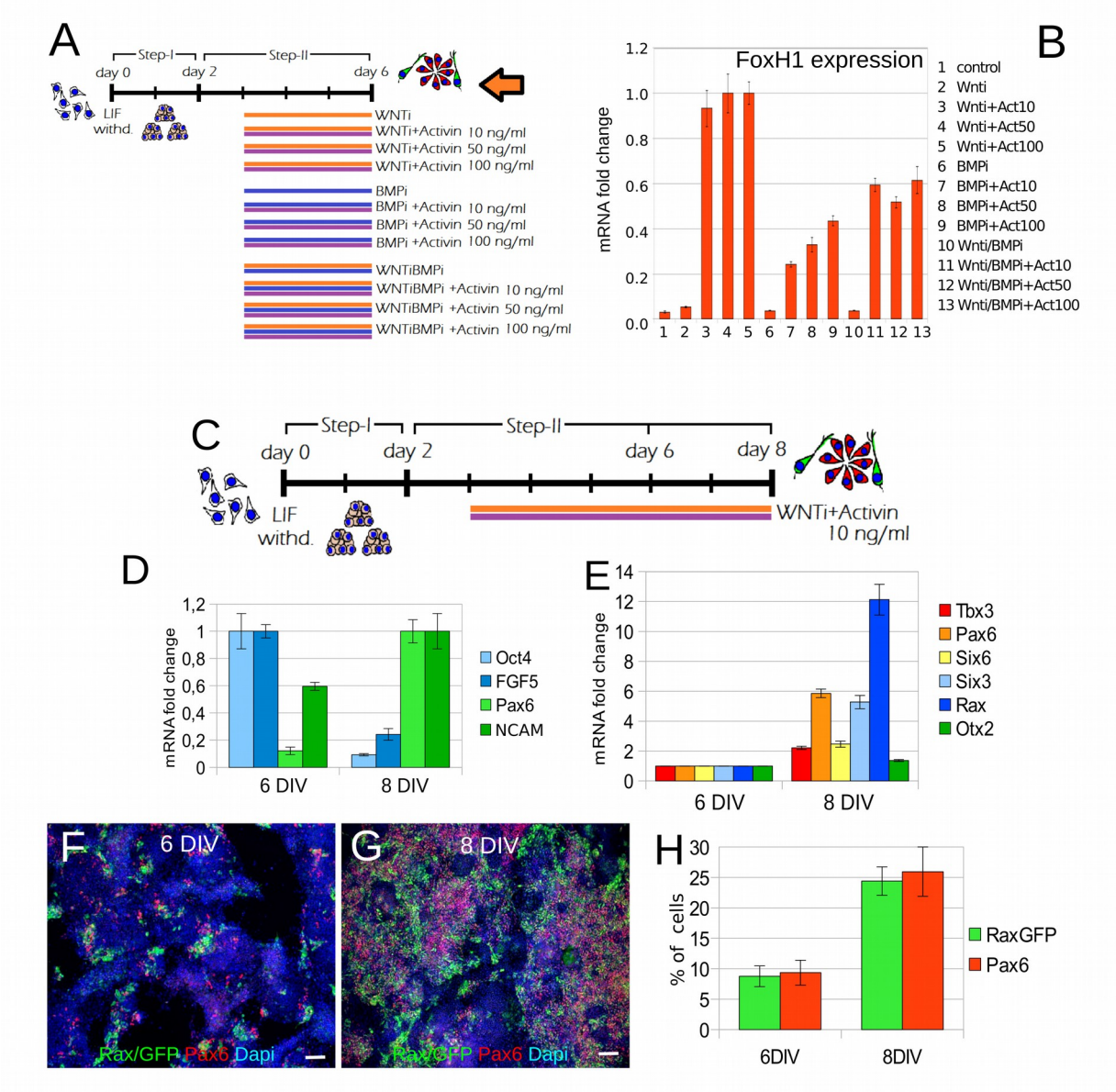

Figure S2, related to Figure 1. Activin signaling activation and time course of neuroectoderm differentiation and *Rax* expression upon Activin treatments of differentiating mESC cultures.

(A) Scheme of Activin, Wnt inhibitor (Wnti) and BMP inhibitor (BMPi) treatments during neuroectoderm differentiation of mESCs. Arrow indicates the time of analysis of *FoxH1* expression (shown in B).

(B) Real time PCR quantification of *FoxH1* expression at 6 DIV in mESCs differentiated in the presence of different combinations of Activin (ACT, 10-100 ng/ml), Wnti and BMPi, as indicated.

Values are normalized to samples with maximal expression levels. ACT, Activin. Ctrl DMSO indicates control culture condition in which 0.1% vehicle was added to CDMM medium. Error bars were obtained from the error propagation formula. (n = 3 independent replicates were pooled together before RNA extraction).

(C) Scheme of mESC neuroectoderm differentiation in the presence of Wnti and Activin. Cells were differentiated as floating aggregates for 2 days and then cultured in adherent conditions until harvesting. Days show the time of mouse ESC differentiation after LIF and serum withdrawal (LIF withd.).

(D,E) Real time PCR quantification of pluripotency (**(D)**, *Oct4*, *FGF5*), neuroectoderm (**(D)**, *Pax6*, *NCAM*) and eye field **(E)** markers in cells differentiated in the presence of Wnti and Activin and harvested at 6 or 8 DIV. Activin-treated cultures show upregulation of neuroectoderm and eye field markers at 8 DIV, while expression of pluripotency markers is transiently maintained until 6 DIV. Values are normalized to samples with maximal expression levels in **(E)** and to the expression in cells at 6 DIV in **(F)**. Error bars were obtained from the error propagation formula. (n = 3 independent replicates were pooled together before RNA extraction).

(F-H) *Rax*/GFP and PAX6 immunocytodetection at 6 or 8 DIV in K/I EB5 cells treated with Activin and Wnti, showing that Activin-treated cultures contain considerable numbers of *Rax*/GFP-positive and PAX6 positive cells at 8 DIV, but not at 6 DIV. **(F,G)** show representative images of PAX6 and *Rax*/GFP staining at 6 DIV **(F)** and 8 DIV **(G)**, while **(H)** reports the quantification of *Rax*/GFP-positive and PAX6-positive cells in these assays. Error bars show the standard error of the mean. Scale bars, 50 microns.

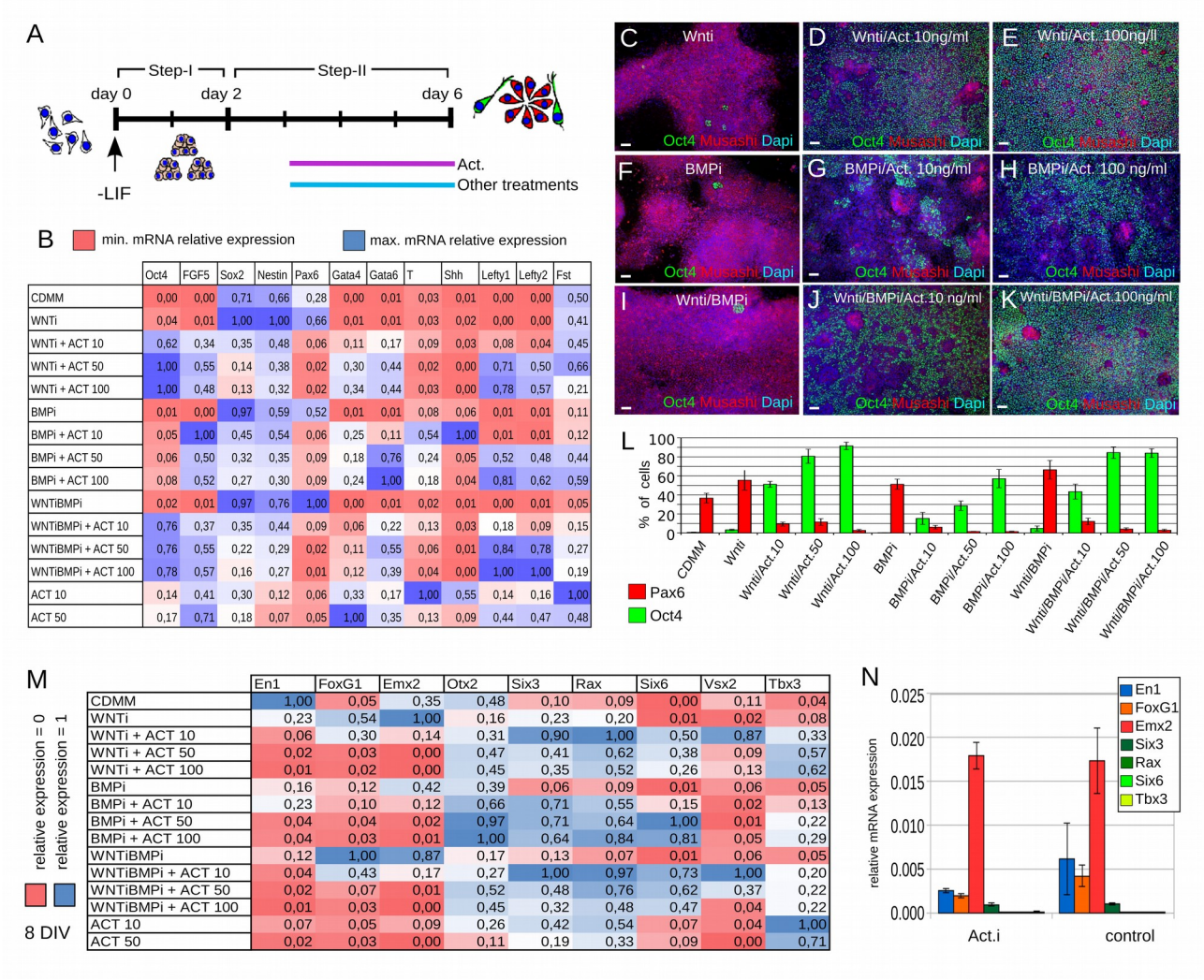

	Oct4	FGF5	Sox2	Nestin	Pax6	Gata4	Gata6	T	Shh	Lefty1	Lefty2	Fst
CDMM	0,00	0,00	0,71	0,66	0,28	0,00	0,01	0,03	0,01	0,00	0,00	0,50
WNTi	0,04	0,01	1,00	1,00	0,66	0,01	0,01	0,03	0,02	0,00	0,00	0,41
WNTi + ACT 10	0,62	0,34	0,35	0,48	0,06	0,11	0,17	0,09	0,03	0,08	0,04	0,45
WNTi + ACT 50	1,00	0,55	0,14	0,38	0,02	0,30	0,44	0,02	0,00	0,71	0,50	0,66
WNTi + ACT 100	1,00	0,48	0,13	0,32	0,02	0,34	0,44	0,03	0,00	0,78	0,57	0,21
BMPi	0,01	0,00	0,97	0,59	0,52	0,01	0,01	0,08	0,06	0,01	0,01	0,11
BMPi + ACT 10	0,05	1,00	0,45	0,54	0,06	0,25	0,11	0,54	1,00	0,01	0,01	0,12
BMPi + ACT 50	0,06	0,50	0,32	0,35	0,09	0,18	0,76	0,24	0,05	0,52	0,48	0,44
BMPi + ACT 100	0,08	0,52	0,27	0,30	0,09	0,24	1,00	0,18	0,04	0,81	0,62	0,59
WNTiBMPi	0,02	0,01	0,97	0,76	1,00	0,00	0,01	0,02	0,01	0,00	0,01	0,05
WNTiBMPi + ACT 10	0,76	0,37	0,35	0,44	0,09	0,06	0,22	0,13	0,03	0,18	0,09	0,15
WNTiBMPi + ACT 50	0,76	0,55	0,22	0,29	0,02	0,11	0,55	0,06	0,01	0,84	0,78	0,27
WNTiBMPi + ACT 100	0,78	0,57	0,16	0,27	0,01	0,12	0,39	0,04	0,00	1,00	1,00	0,19
ACT 10	0,14	0,41	0,30	0,12	0,06	0,33	0,17	1,00	0,55	0,14	0,16	1,00
ACT 50	0,17	0,71	0,18	0,07	0,05	1,00	0,35	0,13	0,09	0,44	0,47	0,48

	En1	FoxG1	Emx2	Otx2	Six3	Rax	Six6	Vsx2	Tbx3
CDMM	1,00	0,05	0,35	0,48	0,10	0,09	0,00	0,11	0,04
WNTi	0,23	0,54	1,00	0,16	0,23	0,20	0,01	0,02	0,08
WNTi + ACT 10	0,06	0,30	0,14	0,31	0,90	1,00	0,50	0,87	0,33
WNTi + ACT 50	0,02	0,03	0,00	0,47	0,41	0,62	0,38	0,09	0,57
WNTi + ACT 100	0,01	0,02	0,00	0,45	0,35	0,52	0,26	0,13	0,62
BMPi	0,16	0,12	0,42	0,39	0,06	0,09	0,01	0,06	0,05
BMPi + ACT 10	0,23	0,10	0,12	0,66	0,71	0,55	0,15	0,02	0,13
BMPi + ACT 50	0,04	0,04	0,02	0,97	0,71	0,64	1,00	0,01	0,22
BMPi + ACT 100	0,04	0,03	0,01	1,00	0,64	0,84	0,81	0,05	0,29
WNTiBMPi	0,12	1,00	0,87	0,17	0,13	0,07	0,01	0,06	0,05
WNTiBMPi + ACT 10	0,04	0,43	0,17	0,27	1,00	0,97	0,73	1,00	0,20
WNTiBMPi + ACT 50	0,02	0,07	0,01	0,52	0,48	0,76	0,62	0,37	0,22
WNTiBMPi + ACT 100	0,01	0,03	0,00	0,45	0,32	0,48	0,47	0,04	0,22
ACT 10	0,07	0,05	0,09	0,26	0,42	0,54	0,07	0,04	1,00
ACT 50	0,02	0,03	0,00	0,11	0,19	0,33	0,09	0,00	0,71

Figure S3, Related to Figure 2. Early Activin treatments cause dose-dependent inhibition of neuroectoderm differentiation and activation of eye field genes.(A) Scheme of treatments with Activin, Wnt inhibition (Wnti) or BMP inhibition (BMPi) during neuroectoderm differentiation of mESCs. Starting from 3 DIV, cells were treated with different combinations of Wnti, BMPi and different doses of Activin (10-100 ng/ml), as indicated, and harvested at 6 DIV for molecular marker analyses.

(B) Color heat map showing the relative expression of markers of pluripotency (*Oct4*, *FGF5*), neuroectoderm differentiation (*Nestin*, *Sox2*, *Pax6*), mesendoderm differentiation (*Gata4-6*, *T*), ventral identity (*Shh*), or secreted antagonists of TGFb family ligands (Lefty1, Lefty2, Follistatin) at 6 DIV in mESCs treated with different combinations and doses of Activin, Wnti or BMPi, as detected by Real time PCR. Values are normalized to minimal (min., 0, red color code) and

maximal (max., 1, blue color code) expression. Activin causes dose-dependent upregulation of pluripotency and mesendoderm genes and downregulation of neuroectoderm genes and these effects are stronger in the absence of Wnti. n = 3 independent replicates were pooled together before RNA extraction.

(C-K) Representative images of OCT4 and Musashi immunocytodetection at 6 DIV, after treatments of differentiating mESCs with moderate (10 ng/ml) or high (100 ng/ml) doses of Activin in combination with Wnti and/or BMPi, as indicated. Activin causes a dose-dependent increase in the numbers of OCT4-positive cells and a corresponding decrease in the numbers of Musashi positive-cells. Scale bars, 50 microns.

(**L)** Quantification of the percentage of cells positive for PAX6 and OCT4 at 6 DIV following similar treatments to those described in **(A, B)** and showed in **(C-K)**, as detected by immunocytodetection. Error bars indicate the standard error of the mean.

(M) Color heat map showing the relative expression, as detected by real time PCR, of markers of neural patterning at 8 DIV following treatments of differentiating mESCs with different combinations and doses of Activin, Wnti or BMPi, as described in SF2. Activin causes more efficient upregulation of eye field genes (*Otx2*, *Six3*, *Rax*, *Six6*, *Vsx2*, *Tbx3*) at moderate doses (10 ng/ml) and in the presence of Wnti, while it represses expression of midbrain (*En1*) and telencephalic (*FoxG1*, *Emx2*) markers at all doses. Values are normalized to minimal (min., 0, red) and maximal (max., 1, blue) expression. n = 3 independent replicates were pooled together before RNA extraction

(N) Real time PCR quantification of neural patterning marker expression at 6 DIV in control cultures (control), or in cultures treated with the Activin/Nodal inhibitor SB431542 (Act. i), showing that Act. i treatments have no effect on the expression of region-specific neural markers. Values are expressed relatively to ß-Actin expression.

Error bars were obtained from the error propagation formula. (n = 3 independent replicates were pooled together before RNA extraction).

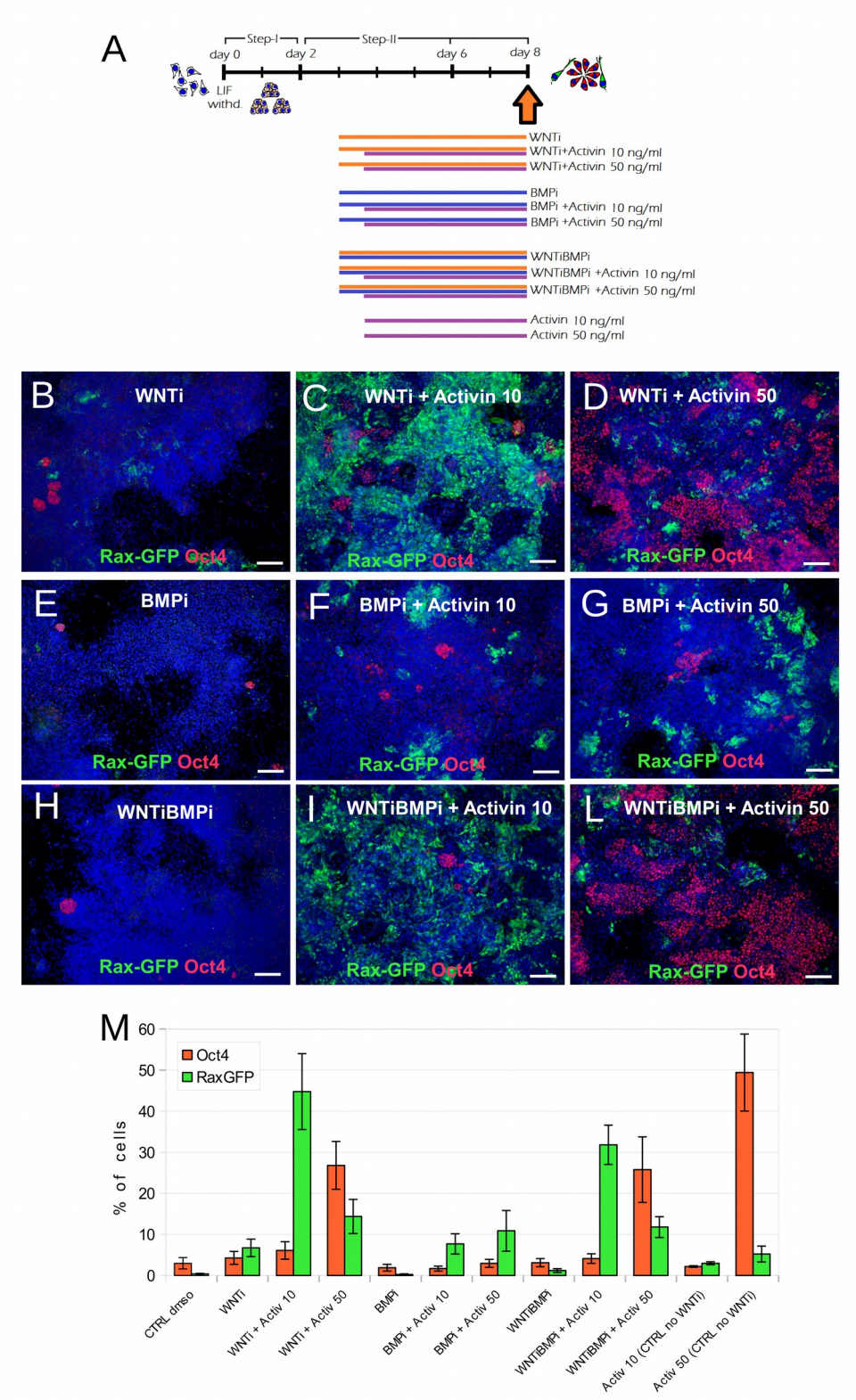

Figure S4, Related to Figure 2. Delayed Activin treatments promote eye field fates at moderate doses.

(A) Scheme of treatments of differentiating mESCs with different combinations of Activin, Wnti or

BMPi. Different doses of Activin (10-50 ng/ml) were added with a 12 hr delay with respect to Wnt and BMP inhibitors.

(B-M) Representative images **(B-L)** and quantification **(M)** of OCT4 and *Rax*/GFP immunocytodetection at 8 DIV in K/I EB5 cells differentiated in the indicated conditions. In the presence of Wnti, Activin supports formation of *Rax*/GFP-positive cells at moderate doses (10 ng/ml) and the maintenance of undifferentiated OCT4-positive cells at higher doses (50 ng/ml). Scale bars, 50 microns. n = 3 independent biological replicates, followed by acquisition and cell counting of n = 6 images per experiment.

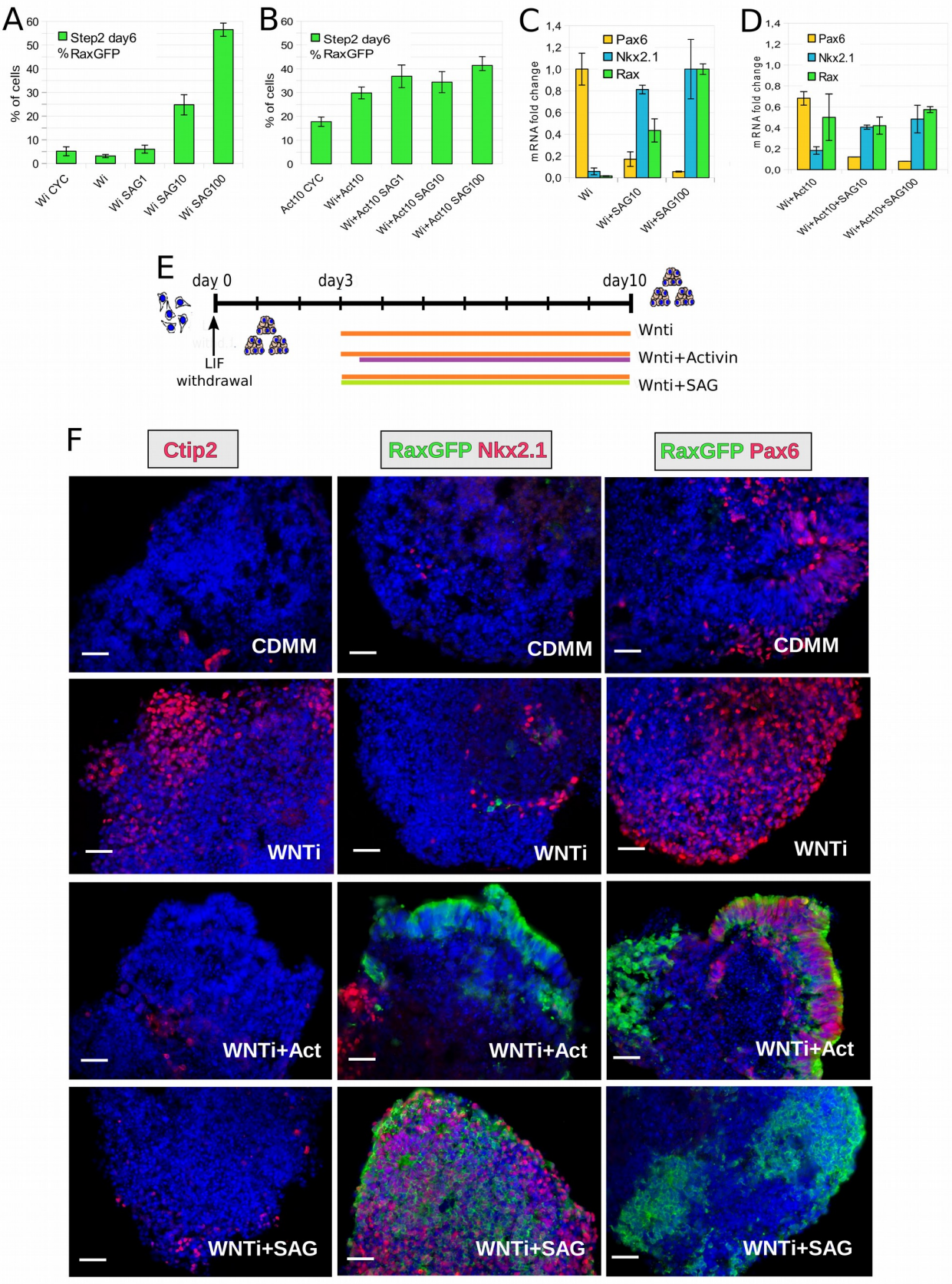
A
Step2 day6
%RaxGFP
% of cells
Wi CYC
Wi
Wi SAG1
Wi SAG10
Wi SAG100
B
Step2 day6
%RaxGFP
% of cells
Act10 CYC
Wi+Act10
Wi+Act10 SAG1
Wi+Act10 SAG10
Wi+Act10 SAG100
C
Pax6
Nkx2.1
Rax
mRNA fold change
Wi
Wi+SAG10
Wi+SAG100
D
Pax6
Nkx2.1
Rax
mRNA fold change
Wi+Act10
Wi+Act10+SAG10
Wi+Act10+SAG100
E
day 0
day3
day10
LIF
withdrawal
Wnti
Wnti+Activin
Wnti+SAG
F
Ctip2
RaxGFP Nkx2.1
RaxGFP Pax6
CDMM
WNTi
WNTi+Act
WNTi+SAG

Figure S5, Related to Figure 3. Activin and SAG promote eye field and ventral hypothalamic fates, respectively.

(A-B) Quantification of *Rax*/GFP-positive K/I EB5 cells as detected by flow-cytometry analysis at 8 DIV following differentiation in the presence of different combination of Wnti (Wi), Cyc, SAG (1-100 nM) or Activin (Act, 10 ng/ml), as indicated. SAG treatments cause dose-dependent increase in the percentage of *Rax*/GFP-positive cells **(A)**. No evident enhancement of *Rax*/GFP expression is detectable in the presence of both Activin and SAG compared to individual treatments **(B)**. Error bars represent s.e.m. (n = 2 independent experiments with n = 3 in vitro technical replicates per experiment; Technical replicates were pooled together and analysed by n = 3 cytometry acquisition each).

(C-D) Real time PCR quantification of *Pax6*, *Nkx2.1* and *Rax* expression at 8 DIV in K/I EB5 cells differentiated in the presence of Wnti **(C)** or Wnti and Activin **(D)**, with or without different doses of SAG (10-100 nM). SAG treatments cause *Pax6* downregulation and *Nkx2.1* and *Rax* upregulation both in the absence or in the presence of Activin. Values are normalized to samples with maximal expression levels. Error bars were obtained from the error propagation formula. (n = 3 independent replicates were pooled together before RNA extraction).

(E) Scheme of treatments with different combinations of Wnti, Activin and SAG of mESC cultures differentiated as floating aggregates until 10 DIV.

(F) Representative images of *Rax*/GFP, CTIP2, NKX2.1 and PAX6 expression as detected by immunocytodetection in mESC aggregates cultured until 10 DIV in the indicated conditions. Activin supports formation of cells expressing *Rax*/GFP and PAX6, while SAG treatments repress PAX6 and increase *Rax* and NKX2.1 expression. Lower numbers of cells expressing CTIP2 (a marker of cortical differentiation) are detectable in aggregates treated with Activin or SAG compared to treatments with Wnti only. Scale bars: 30 microns.

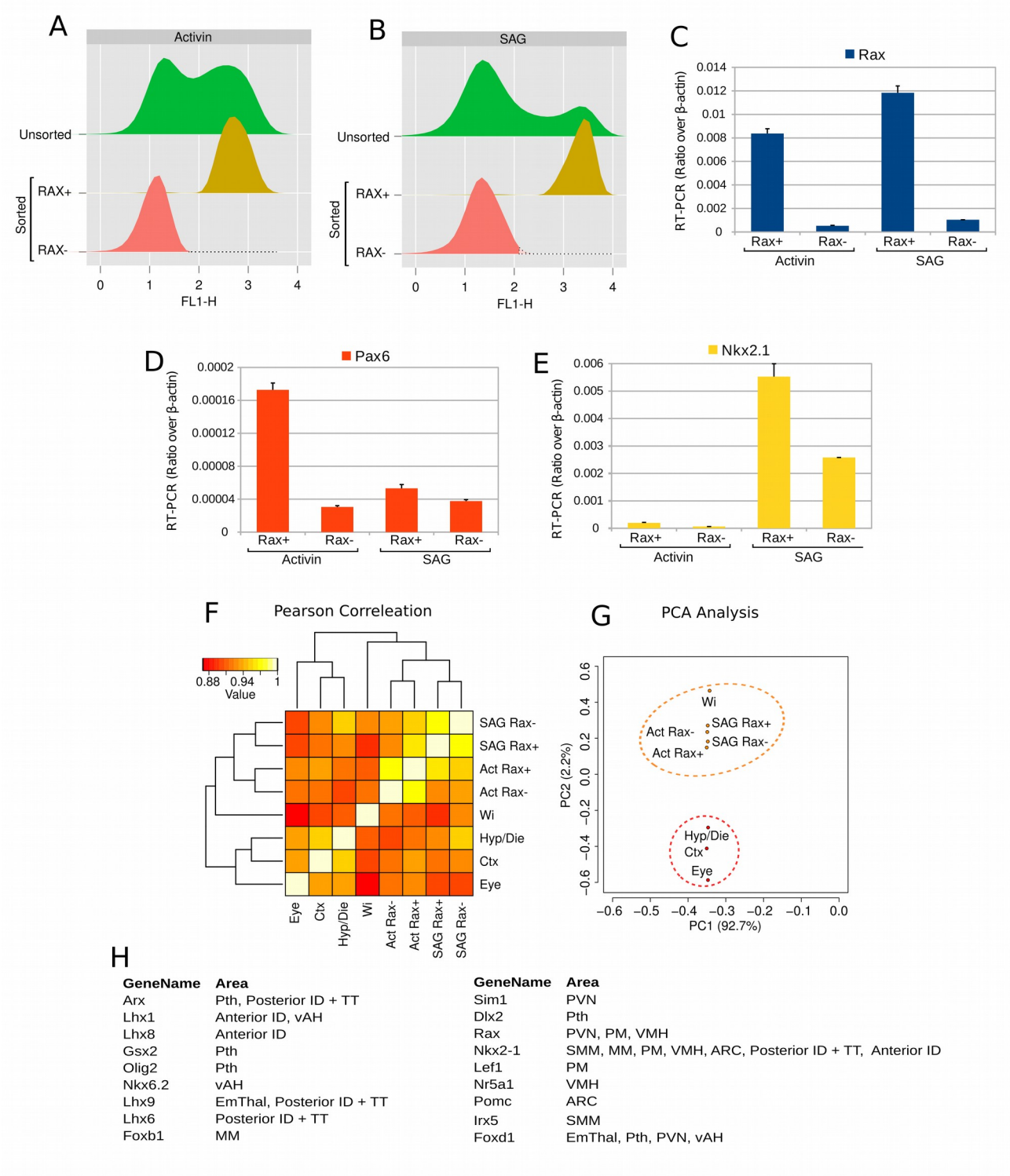

GeneName	Area	GeneName	Area
Arx	Pth, Posterior ID + TT	Sim1	PVN
Lhx1	Anterior ID, vAH	Dlx2	Pth
Lhx8	Anterior ID	Rax	PVN, PM, VMH
Gsx2	Pth	Nkx2-1	SMM, MM, PM, VMH, ARC, Posterior ID + TT, Anterior ID
Olig2	Pth	Lef1	PM
Nkx6.2	vAH	Nr5a1	VMH
Lhx9	EmThal, Posterior ID + TT	Pomc	ARC
Lhx6	Posterior ID + TT	Irx5	SMM
Foxb1	MM	Foxd1	EmThal, Pth, PVN, vAH

Figure S6, Related to Figure 4. Transcriptomic analyses on sorted *Rax*+ and *Rax*- cells from cultures treated with Activin or SAG.

(A,B) Flow-cytometry analysis of K/I EB5 cells treated with Activin or SAG as indicated in Fig. 3A

and sorted at DIV10.

(C-E) Expression levels of *Rax* **(C)**, *Pax6* **(D)** and *Nkx2.1* **(E)**, as evaluated by qRT-PCR in sorted *Rax*+ and *Rax*- cells from cultures treated with Activin or SAG.

(F) Clustering analysis, showing the distribution of Pearson Correlation among the entire transcriptomes of different cell cultures and embryonic brain tissues. ActA, Activin A; Ctx, Cortex; Hyp/Die, Hypothalamus/Diencephalon; *Rax*+ and *Rax*-, sorted K/I EB5 cells positive or negative for GFP expression, respectively; SAG, SHH Agonist; Wi, Wnt inhibition .

(G) PCA of samples as in **(F)**. PC1 and PC2 indicate first and second principal component, respectively.

(H) Subsets of markers that identify distinct hypothalamic and/or prethalamic regions, as previously described (Shimogori et al., 2010). SMM, supramamillary nucleus; MM, mamillary nucleus; PM, premamillary region; VMH, ventromedial hypothalamic nucleus; ARC arcuate nucleus; ID, intrahypothalamic diagonal region; TT, tuberomamillary terminal region; PVN, paraventricular nucleus; Em Thal, eminentia thalami; PTh, prethalamus; vAH,ventral anterior hypothalamus.

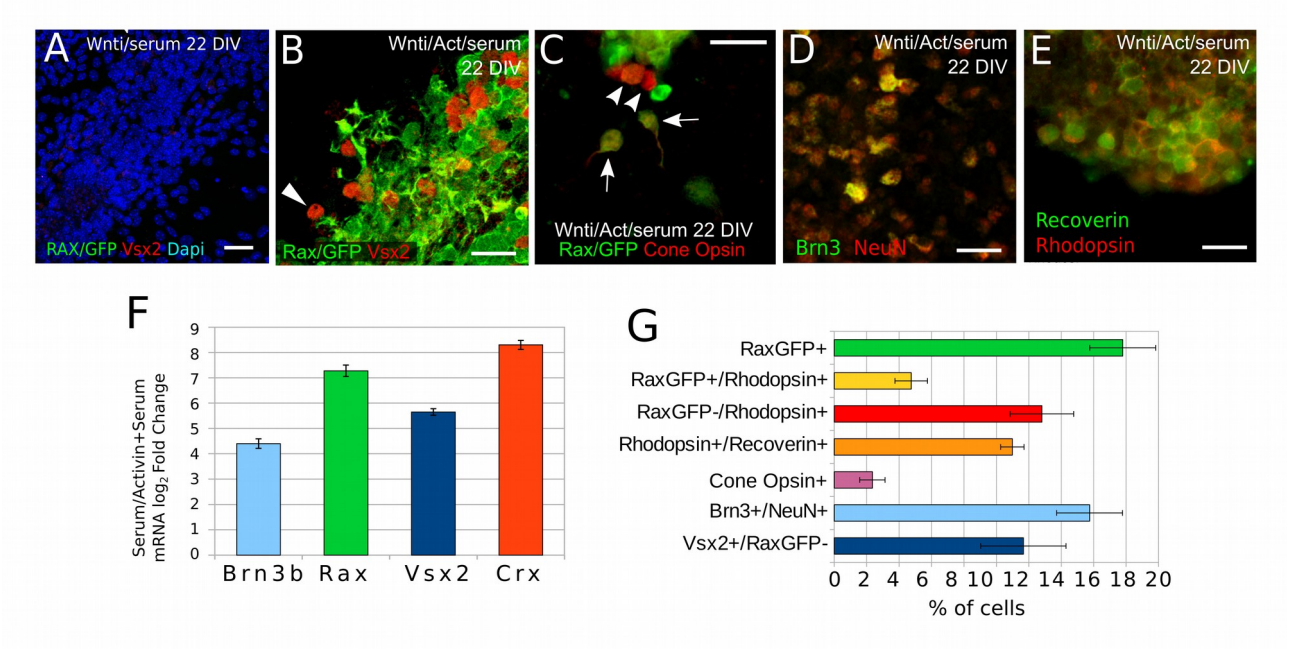

Figure S7, Related to Figure 5. Activin treatments lead to the expression of markers of retinal neuronal cell types in long-term cultures.(A,E) Representative images of K/l EB5 cells differentiated in the indicated conditions and immunostained for both Vsx2 and GFP (**A-B**), Cone Opsin and GFP (**C**), BRN3 and NeuN (**D**), Rhodopsin and Recoverin (**E**) at 22 DIV. Arrowheads in (**B,C**) point to GFP-negative cells that express Vsx2 or Cone Opsin, respectively. Arrows in C indicate double-positive GFP/Cone Opsin cells . Scale bars: 10 microns.

(F) Induction of retinal ganglion cell (*Brn3b*), bipolar cell (*Vsx2*), photoreceptor (*Crx*) or retinal progenitor (*Rax*) markers, as detected at 22 DIV by Real time RT-PCR quantification in cells treated with Wnti/activin compared to cell treated with Wnti. Retinal differentiation markers are upregulated in Activin-treated cultures compared to the Wnti-only condition. After 8 DIV, culture medium was supplemented with 2% Fetal Bovine Serum (Ser) to support cell survival. Error bars were obtained from the error propagation formula. n = 3 in vitro technical replicates were pooled together before RNA extraction. (G) Ratios of different cell types in Wnti/Activin/serum-treated cells at DIV22. Error bars show the standard error of the mean. (n = 2 independent experiments).

SUPPLEMENTAL EXPERIMENTAL PROCEDURES

Mouse embryonic stem cell culture

Murine ES cell lines E14Tg2A (passages 25-38) and K/l-EB5 (transgenic *Rax*-GFP ES cells, used with the kind permission of Y. Sasai, Riken Center, Japan) were cultured on gelatin-coated tissue culture dishes at a density of 40,000 cells/cm2. ES cell medium, which was changed daily, contained GMEM (Sigma), 10% Fetal Calf Serum, 2mM Glutamine, 1mM sodium Pyruvate, 1mM non-essential amino acids, 0.05mM β-mercaptoethanol, 100 U/ml Penicillin/Streptomycin and 1000 U/ml recombinant mouse LIF (Invitrogen).

Chemically defined minimal medium (CDMM) for neural induction consisted of DMEM/F12 (Invitrogen), 2mM Glutamine, 1mM sodium Pyruvate, 0.1mM non-essential amino acids, 0.05mM β-mercaptoethanol, 100 U/ml Penicillin/Streptomycin supplemented with N2/B27 (no vitamin A; Invitrogen). The protocol of ES neuralization consisted of two steps. In Step-I, dissociated ES cells were washed with DMEM/F12, aggregated in agar-coated culture dishes (65,000 cells per cm2) and cultured as floating aggregates in CDMM for 2 days. The second day, 75% of CDMM was renewed. In Step-II, ES cell aggregates were dissociated and cultured in adhesion (65,000 cells per cm2) on Poly-ornithine (Sigma; 20 µg/ml in sterile water, 24 hours coating at 37°C) and natural mouse Laminin (Invitrogen; 2.5 µg/ml in PBS, 24 hours coating at 37°C) for 4/6 days, changing CDMM daily. Serum employed for Trypsin inactivation was carefully removed by several washes in DMEM/F12. To investigate the expression of late markers, Step-II was prolonged when needed, until a maximum of 22 days, without any additional dissociation/replating; for late term cultures, 50% of the medium was renewed daily, and 2% Fetal Bovine Serum (FBS) was added to colture medium starting at 8-10 DIV to promote cell survival. For late term retinal differentiation, better results were obtained when culturing cells on a glass coated surface, compared to culture on plastic plates (data not shown).

Human embryonic stem cell culture

H9 (WiCell Inc., Madison, Wisconsin, USA) hESCs (55-69 passages) were maintained on irradiated mouse embryonic fibroblasts (MEFs) in KSR medium containing KO-DMEM supplemented with 20% Serum Replacement (Invitrogen), 1 mM glutamine, 0.1 mM ß-mercaptoethanol, 1% nonessential aminoacid stock and 4 ng/ml FGF2 following published protocols (Schatten, Smith, Navara, Park, & Pedersen, 2005). hESC differentiation was induced by culture in floating aggregate non-adherent conditions in chemically defined medium (CDM) as previously described (Vallier, Reynolds, & Pedersen, 2004). The composition of CDM was 50% IMDM (Invitrogen) plus 50% F12 NUT-MIX (Invitrogen), supplemented with 7 µg/ml of Insulin, 15 µg/ml of Transferrin, 450 µM of monothioglycerol, 1% chemically-defined lipid concentrate

(Invitrogen) and 5 mg/ml bovine serum albumin fraction V. Floating aggregates were cultured in plain CDM or in CDM containing 50 ng/ml Activin for 12-14 days, followed by lysis in RLT buffer (Qiagen) for total RNA purification and real time PCR. Alternatively, cell aggregates were fixed overnight in 4% paraformaldehyde in PBS at 4ºC and stored in methanol at -20ºC for *in situ* hybridization. Real time PCR and *in situ* hybridization analyses were performed as previously described (Lupo et al., 2013; J. R. Smith et al., 2008).

Growth factor and morphogen treatments on mouse ES cells

The following factors were tested by addition during Step-II, as indicated in the text: Dorsomorphin (BMP signaling inhibitor; Sigma-Aldrich P5499; 5 µM), Cyclopamine (SHH signaling inhibitor; Sigma-Aldrich C4116; 5 µM), SAG (SHH agonist; Santa Cruz Biotechnology sc-212905; from 1 to 100 nM), SB431542 (TGFbeta-signaling inhibitor; Sigma-Aldrich S4317; 10 µM), IWR-1-Endo (Wnt inhibitor; Calbiochem 681669; 5/10 µM) and Recombinant Human/Mouse/Rat Activin-A (R&D 338-AC-005; ranging from 10 to 100 ng/ml).

Semiquantitative real-time PCR

Total RNA was extracted from mouse ES cell with NucleoSpin RNA II columns (Macherey-Nagel). ES cells from at least two-three different wells of 24-well plates were always pooled together to compensate for variability in cell seeding. RNA quantity and RNA quality were assessed with Nanodrop and gel electrophoresis. For each sample, 200/500 ng of total RNA were reverse-transcribed. Amplified cDNA was quantified using GoTaq qPCR Master Mix (Promega) on Rotor-Gene 6000 (Corbett). Amplification take-off values were evaluated using the built-in Rotor-Gene 6000 relative quantitation analysis function, and relative expression was calculated with the $2^{-\Delta\Delta Ct}$ method, normalizing to the housekeeping gene β-Actin. Standard errors were obtained from the error propagation formula as described in (Nordgård, Kvaløy, Farmen, & Heikkilä, 2006) and statistical significance was probed with randomization test, taking advantage of REST Software (Pfaffl, Horgan, & Dempfle, 2002). Primers used are listed below.

Activin-A	sense	AGGGCCGAAATGAATGAAC
Activin-A	antisense	ACTTCTGCACGCTCCACTAC
Brn3	sense	TCCCTGTCTCCCTCCTTTG
Brn3	antisense	TCTCTTCCTTTCTTCTGGGATTT
Crx	sense	ACCAGGCTGTCCCATACTCA
Crx	antisense	TCGCCCTACGATTCTTGAAC
Ctip2	sense	CCCGACCCTGATCTACTCAC
Ctip2	antisense	CTCCTGCTTGGGACAGATGC
Emx2	sense	GGCTAGAGCACGCTTTTGAG

Emx2	antisense	CACCGGTTAATGTGGTGTGT
En1	sense	AGTGGCGGTGGTAGTGGA
En1	antisense	CCTTCTCGTTCTTTTTCTTCTTT
FGF5	sense	GTCAATGGCTCCCACGAA
FGF5	antisense	TGGAATCTCTCCCTGAACTTACA
Follistatin	sense	GGGATTCCAAGGTTGGCAGA
Follistatin	antisense	TCCGAGATGGAGTTGCAAGAT
FoxG1	sense	CGACCCTGCCCTGTGAGT
FoxG1	antisense	GGAAGAAGACCCCTGATTTTG
FoxH1	sense	CGCCACAACCTTTCCTCTAA
FoxH1	antisense	GGAATCAGGCTCACATCCAC
Gata4	sense	GGAAGACACCCCAATCTCG
Gata4	antisense	CATGGCCCCACAATTGAC
Gata6	sense	ACTCGCCCTACATGGCCGCA
Gata6	antisense	TAAGCTGTGGAGCACCGGCG
Id1	sense	CGACTACATCAGGGACCTGCA
Id1	antisense	GAACACATGCCGCCTCGG
Irx3	sense	AGTGCCTTGGAAGTGGAGAA
Irx3	antisense	CGAGGAGAGAGCTGATAAGACC
Lefty1	sense	CCTGTGTGTGCTCTTTGCTTC
Lefty1	antisense	GGCAATTGGGGATTCTGTCCT
Lefty2	sense	CTCAGATGGGGCGCTCATAC
Lefty2	antisense	AGCAAAGGTCTGACGAGAGC
NCAM	sense	AGGAGAAATCAGCGTTGGAG
NCAM	antisense	CGATGTTGGCGTTGTAGATG
Nestin	sense	TGTCCCTTAGTCTGGAAGTGG
Nestin	antisense	GGGGAAGAGAAGGATGTTGG
Nkx2.1	sense	CAATGAGGCTGACGCCCCCG
Nkx2.1	antisense	GAAGTGGGTTTCCTGTCTGAGCG
Nodal	sense	GAGGGCGAGTGTCCTAACC
Nodal	antisense	ATGCTCAGTGGCTTGGTCTT
Oct4	sense	TCAGCTTGGGCTAGAGAAGG
Oct4	antisense	GGCAGAGGAAAGGATACAGC
Otx2	sense	CCACTTCGGGTATGGACTTG
Otx2	antisense	GGTCTTGGCAAACAGAGCTT
Pax6	sense	CCTCCTTCACATCAGGTTCC
Pax6	antisense	CATAACTCCGCCCATTCACT
Rax	sense	AAGACGGCATCCTAGACACCT
Rax	antisense	GTGCTTCTCCTTGCTCCTTG
SatB2	sense	CATGAGCCCTGGTCTTCTCT
SatB2	antisense	AACTGCTCTGGGAATGGGTG
Shh	sense	CAGAGGGAACGAACGAGCCGA
Shh	antisense	CACCAGCAGCGAGGAAGCAAGGAT

Six3	sense	TCAACAACCCCACCACCACCTACT
Six3	antisense	CACCTCTTTTATGCTTTCTGCCCGC
Six6	sense	CAAAAACCGCAGACAAAGAGA
Six6	antisense	GTCGCTGGATGTGATGGAG
Sox2	sense	ACTTTTGTCCGAGACCGAGA
Sox2	antisense	CTCCGGGAAGCGTGTACTTA
T (Brachyury)	sense	TACACACCACTGACGCACACGG
T (Brachyury)	antisense	GCAGCCCCTTCATACATCGGAG
Tbr1	sense	CGCCCTCCTCCATCAAATCCATCG
Tbr1	antisense	GCAGTTCTTCTCGCAGTCCCGC
Tbx3	sense	ACAAGCGGGGTACAGAGATG
Tbx3	antisense	ACCATCCACCGAGAGTTGTG
Vsx2	sense	CCAGTGACCGAAAAATGTCC
Vsx2	antisense	ACATCTGGGTAGTGGGCTTC
β-Actin	sense	AATCGTGCGTGACATCAAAG
β-Actin	antisense	AAGGAAGGCTGGAAAAGAGC

Immunocytodetection

Cells prepared for immunocytodetection experiments were cultured on Poly-ornithine/Laminin coated round glass coverslips. Cells were fixed using 2% paraformaldehyde for 10-15 minutes, washed twice with PBS, permeabilized using 0.1% Triton X100 in PBS and blocked using 0.5% BSA in PBS. Primary antibodies used for microscopy included OCT3/4 (1:200; Santa Cruz DBA sc-5279), Musashi-1 (1:200; Cell Signaling), Nestin (1:200; Millipore MAB353), FOXG1 (1:200; Abcam ab18259), CTIP2 (1:400; Abcam ab28448), GAD65 (1:500; Chemicon MAB351), PAX6 (1:400; Covance PRB-278P), NKX2.1 (1:400; Abcam ab76013), GFP (rabbit polyclonal, 1:1000, Invitrogen A6455; or chicken polyclonal, 1:1000, Aves Lab GFP-1020), Rhodopsin (1:1000; Sigma O4886), Recoverin (1:500; Millipore AB5585), Opsin red/green (1:1000; Millipore AB5405), BRN3a (1:100; Millipore AB5945), NeuN (1:1000; Millipore MAB377), β-III-Tubulin (1:1000; Covance MRB435P) and Vsx2 (1:200; Exalpha X1180P). Primary antibodies were incubated 2 hours at room temperature; cells were then washed three times with PBS (10' each). Alexa Fluor 488 and Alexa Fluor 568 anti-mouse, anti-rabbit or anti-chicken IgG conjugates (Molecular Probes A28175, A-11008, A-21441, A-21124, A-11061 and A-11041, 1:500) were incubated 1 hr at RT in PBS containing 0.1% Triton X100 and 0.5% BSA for primary antibody detection, followed by three PBS washes (10' each). Nuclear staining was obtained with DAPI. The same protocol was applied on sections of embryoid bodies after fixation (2 hours at 4°C in 2% PFA), dehydration (O/N at 4°C in 30% sucrose), inclusion in OCT and cryostat sectioning.

In situ hybridization

Digoxigenin (DIG)-labeled sense and antisense RNA probes were generated for human *OCT4*,

RAX, *OTX2*, *PAX6* and *VSX2* plasmids, as described (W. C. Smith & Harland, 1991). *In situ* whole-mount hybridization on human embryoid bodies was carried out as described (Thisse & Thisse, 2008), with few modifications. Briefly, embryoid bodies were rehydrated in PBST series and treated with Proteinase K (Sigma; 1:2000 dilution in PBST, 20'), then fixed in 4% PFA for 30'. After several washes in PBST, embryoid bodies were pre-incubated in hybridization solution (HYB; 5x SSC, 50% Formamide, 50mg/ml torula RNA, 100mg/ml Heparin, 20% Tween-20, 1M Citric acid) for 6 hours at 65°C, then incubated O/N with HYB plus RNA probes (500ng probe in 1 ml HYB solution). The day after, the samples underwent several washes in HYB, then in 2X SSC and in 0.2X SSC at 65°C, and finally in PBST at room temperature. Embryoid bodies were then preblocked in MAB plus 2% blocking reagent (Roche) for 2 hours at room temperature, and incubated O/N at 4°C with anti-DIG antibody (1:5000; Roche). Signal detection with BMPurple (Roche) was performed according to manufacturer's instructions; 2 quick washes with Tetramisole (0.5 mg/ml; Sigma) were performed before staining to reduce background. To fix colors, samples were incubated in 4% PFA for 30' at room temperature, washed with PBS and stored at 4°C.

Microarray hybridization and data analysis

Tissues (Cortex, Hypothalamus/Diencephalon and Eye) were dissected from n = 3 mouse embryos (Sv129s6 strain, Taconic) at embryonic day (E)12.5. Cells were detached by trypsinization, washed and resuspended in PBS, 2% FBS, 2mM EDTA and kept on ice. *Rax*::GFP+ and *Rax*::GFP- populations were separated on a S3 Cell sorter (Biorad). Total RNA was extracted with NucleoSpin RNA II columns (Macherey–Nagel). RNA from three different sets of experiments was pooled. RNA quality was assessed with Agilent Bioanalyzer RNA 6000 Nano kit; 50 ng of RNA were labeled with LowInput QuickAmp Labeling Kit One-Color (Agilent Technologies), purified and hybridized overnight onto Agilent SurePrint G3 Mouse Gene Expression Array (8x60K), according to the manufacturer's instructions. Agilent Microarray scanner G2564C was used for slide acquisition and spot analysis was performed with Feature Extraction software (Agilent). Data were background-corrected and normalized between arrays by means of Bioconductor package limma (Smyth, 2005). Principal component analysis (PCA) and hierarchical clustering were performed both on whole-gene expression datasets or on the top 2% genes (n=414) displaying the higher variance among samples.

ChIP-seq data reanalysis

Raw ChIP-seq data were downloaded as SRA files from NCBI Gene Expression Omnibus (GEO, http://www.ncbi.nlm.nih.gov/geo/), converted into Fastq files and aligned to reference mouse (GRCh36/mm8) and human (GRCh37/hg19) genomes using Bowtie (Langmead, Trapnell, Pop, & Salzberg, 2009). Taking advantage of rsem-bam2wig program

(http://deweylab.biostat.wisc.edu/rsem/), alignments were converted to Wiggle Track Format in order to be loaded and visualized as gene plots in UCSC Genome Browser (Kent et al., 2002).

SUPPLEMENTAL REFERENCES

Kent, W. J., Sugnet, C. W., Furey, T. S., Roskin, K. M., Pringle, T. H., Zahler, A. M., & Haussler, a. D. (2002). The Human Genome Browser at UCSC. *Genome Research*, *12*(6), 996–1006.

Kim, S. W., Yoon, S.-J., Chuong, E., Oyolu, C., Wills, A. E., Gupta, R., & Baker, J. (2011). Chromatin and transcriptional signatures for Nodal signaling during endoderm formation in hESCs. *Developmental Biology*, *357*(2), 492–504.

Langmead, B., Trapnell, C., Pop, M., & Salzberg, S. L. (2009). Ultrafast and memory-efficient alignment of short DNA sequences to the human genome. *Genome Biology*, *10*(3), R25.

Lupo, G., Novorol, C., Smith, J. R., Vallier, L., Miranda, E., Alexander, M., … Harris, W. A. (2013). Multiple roles of Activin/Nodal, bone morphogenetic protein, fibroblast growth factor and Wnt/β-catenin signalling in the anterior neural patterning of adherent human embryonic stem cell cultures. *Open Biology*, *3*(4), 120167.

Mullen, A. C., Orlando, D. A., Newman, J. J., Lovén, J., Kumar, R. M., Bilodeau, S., … Young, R. A. (2011). Master transcription factors determine cell-type-specific responses to TGF-β signaling. *Cell*, *147*(3), 565–76.

Nordgård, O., Kvaløy, J. T., Farmen, R. K., & Heikkilä, R. (2006). Error propagation in relative real-time reverse transcription polymerase chain reaction quantification models: the balance between accuracy and precision. *Analytical Biochemistry*, *356*(2), 182–93.

Pfaffl, M. W., Horgan, G. W., & Dempfle, L. (2002). Relative expression software tool (REST) for group-wise comparison and statistical analysis of relative expression results in real-time PCR. *Nucleic Acids Research*, *30*(9), e36. Retrieved from

Schatten, G., Smith, J., Navara, C., Park, J.-H., & Pedersen, R. (2005). Culture of human embryonic stem cells. *Nature Methods*, *2*(6), 455–63.

Shimogori, T., Lee, D. a, Miranda-Angulo, A., Yang, Y., Wang, H., Jiang, L., Yoshida, A.C., Kataoka, A., Mashiko, H., Avetisyan, M., et al. (2010). A genomic atlas of mouse hypothalamic development. Nat. Neurosci. 13, 767–775.

Smith, J. R., Vallier, L., Lupo, G., Alexander, M., Harris, W. A., & Pedersen, R. A. (2008). Inhibition of Activin/Nodal signaling promotes specification of human embryonic stem cells into neuroectoderm. *Developmental Biology*, *313*(1), 107–17.

Smith, W. C., & Harland, R. M. (1991). Injected Xwnt-8 RNA acts early in Xenopus embryos to promote formation of a vegetal dorsalizing center. *Cell*, *67*(4), 753–65.

Smyth, G. K. (2005). Limma : Linear Models for Microarray Data. *Bioinformatics*, (2005), 397–420.

Thisse, C., & Thisse, B. (2008). High-resolution in situ hybridization to whole-mount zebrafish embryos. *Nature Protocols*, *3*(1), 59–69.

Vallier, L., Reynolds, D., & Pedersen, R. A. (2004). Nodal inhibits differentiation of human embryonic stem cells along the neuroectodermal default pathway. *Developmental Biology*, *275*(2), 403–21.